NUMERICAL INVESTIGATION OF NANOFLUID FLOW AND HEAT TRANSFER IN FLAT PLATE SOLAR COLLECTOR

By

NAI-JEI TANG

A thesis submitted to the

School of Graduate Studies

Rutgers, The State University of New Jersey

In partial fulfillment of the requirements

For the degree of

Master of Science

Graduate Program in Mechanical and Aerospace Engineering

Written under the direction of

Professor Zhixiong Guo

And approved by

_____

_____

_____

_____

New Brunswick, New Jersey

[October 2020]

ABSTRACT OF THE THESIS

NUMERICAL INVESTIGATION OF NANOFLUID FLOW AND HEAT TRANSFER IN FLAT PLATE SOLAR COLLECTOR

by

NAI-JEI TANG

Thesis Director:

Dr. Zhixiong Guo

Since the industrial revolution, fossil fuel has been the main resource for generating power and energy. However, with an increase in environmental awareness, people realized the huge negative impact of fossil fuel burning on Earth. Consequently, the concept of renewable energy emerged, and the field of renewable energy has seen an increasing number of researchers devote effort to solving the energy crisis facing humanity. Among all the renewable energy sources, solar energy plays one of the important role in the development of industry. Google Scholar shows that has been a huge amount of research for generating innovative ideas for improving the efficiency of the solar collector with the objective of reducing reliance on fossil fuel. In 1995, Choi and Eastman introduced the concept of nanofluid, which is obtained by adding high-

conductivity nanoparticles to a base fluid; the nanoparticle addition enhances the thermal conductivity and heat transfer capability of the fluid.

In this study, the commercial software COMSOL Multiphysics was used to model nanofluid flow and heat transfer in the tube of a flat plate solar collector. The flow in the tube is laminar. Two types of nanoparticles, i.e., Al_2O_3 and CuO, with three different volume concentrations, i.e., 0%, 0.5%, and 1% in water, were chosen for comparison purposes. The inlet temperature of the fluid was assumed to be uniform at the room temperature of 298 K.

In this thesis, the results of a simulation are discussed in terms of three parameters: outlet temperature, efficiency, and pressure drop. The outlet temperature of the nanofluid was greater than that of pure water, and the difference increased with the volume concentration of the nanoparticles. Furthermore, the water-based CuO nanofluid has better performance than the water-based Al_2O_3 nanofluid. The efficiency of the solar collector did not increase when nanoparticles were added, owing to limitations of the model; an example of a limitation is that solar energy absorption by nanoparticles was not considered in the model. However, the efficiency of the solar collector increased noticeably with an increase in the mass flow rate. The volume flow rate was used instead of the mass flow rate for comparing the pressure drop. The simulation results showed that the pressure drop of both fluids increased with the volume concentration of the nanoparticles, and that the difference in the pressure drop between the CuO and Al_2O_3 nanofluids was not apparent.

Acknowledgments

First of all, I would like to thank my thesis advisor Professor Z. Guo of the Department of Mechanical and Aerospace Engineering, Rutgers University-New Brunswick for providing me with an opportunity to complete my master's thesis. Not only has he never hesitated to teach me something new or solve my problem during my research, he has also made me a better student and researcher.

I express my gratitude to my parents who have supported me financially. I could not have achieved anything without their backup. I also need to appreciate the encouragement provided by my girlfriend Hsiao-Wei Tung who was always there to cheer me up during my study. It would have been impossible to complete this thesis without her support, and I would like to thank her.

Author

Nai-Jei Tang

Nomenclature

A	Area of absorber plate	m^2
C_P	Specific heat coefficient of fluid	J/kg K
D	Diameter of tube	m
d_{bc}	Channel thickness	m
d_z	Depth in z-direction	m
F	Volume force	N/m^3
g	Gravity	N/kg
h	Convection heat transfer coefficient	-
K	Thermal conductivity	W/m K
L	Length of tube	m
m	Mass	kg
$\dot{m}$	Mass flow rate	kg/s
Q_b	General heat source	W/m^2
Q_{rec}	Total energy received by solar collector	W
Q_{abs}	Energy absorbed in the solar collector system	W
$q''or\ q$	Heat flux	W/m^2
S	Surface area	m^2
T_{amb}	Ambient temperature	K
T_{in}	Inlet temperature of solar collector	K
T_{out}	Outlet temperature of solar collector	K

u	Velocity vector	m/s
Greek Symbols		
ΔP	Pressure drop	Pa
ρ	Density of fluid	kg/m^3
$\emptyset$	Volume fraction of nanoparticles	vol%
μ	Viscosity of fluid	Pa·s
η	Efficiency	
Subscripts		
amb	Ambient	-
abs	Absorbed in system	-
avg	Average	-
b	Boundary	-
bc	Boundary condition	-
bf	Base fluid	-
in	Inlet	-
nf	Nanofluid	-
out	Outlet	-
P	Pump	-
rec	Received by solar collector	-
ref	Reference	-

Table of Contents

List of Figures

List of Tables

Chapter I

Introduction

1.1 Solar Energy

Since the industrial revolution, fossil fuel has been the primary source of energy, and it has been a major contributor to environmental pollution. According to a report of the U.S. Energy Information Administration [1], about 63% of the total electricity generated in the USA in 2019 was from fuel fossil, which includes coal, petroleum, natural gas, and other gases, about 20% was from nuclear power, and about 17% was from renewable energy sources.

With an increase in environmental awareness, people realized that fossil fuel combustion for electricity generation caused damage to the environment. Every government is actively seeking solutions to solve their future alternative energy sources for satisfying their energy requirements. Solar energy is one of the renewable energy sources. It can be used for generating electricity, and it is one of the cleanest and most abundant renewable energy sources. According to the SEIA website, the United States has 71 GW of solar energy capacity, which can provide power to more than 13.5 million homes [2]. Boyle [3] pointed out that five countries use solar power the most. China, in the first place, has 130 GW of solar energy capacity and holds the largest operational project or solar power in the world; The second, third, fourth and fifth are occupied by the United States, Japan, Germany, and India, respectively.

Currently, the most challenging tasks are enhancing the efficiency of solar power generation and storing solar energy efficiently. The solar intensity varies with location, and therefore some areas are more suitable for producing solar power, while some others are not favorable. According to the National Renewable Energy Laboratory, the solar intensity in the Mojave Desert is twice that in the Pacific Northwest, which implies that the Mojave Desert is suitable for producing more electricity from solar energy [4]. More research on the material of the PV cells and the design of solar collectors is required for increasing solar power generation.

1.2 Solar Collectors

There are several types of solar collectors, including flat plate solar collectors (FPSCs), evacuated tube collectors, line focus collectors, and point focus collectors [5]. Each type of solar collector has its uniqueness. Line focus collectors and point focus collectors can provide solar power with high efficiency. However, both collectors are costly, and a huge space is required for their installation. The evacuated tube collector is one of the most efficient solar collectors, and it can operate well in freezing climates; however, a disadvantage is that it is the most expensive type of hot water solar collector [6].

Some solar collectors transform solar energy into heat, which is transferred to a working fluid. Such a system is called solar water heating (SWH) [7]. The working fluid in solar collector is mostly water.

1.3 Nanofluid

Recently, researchers have been exploring the use of alternative materials as the working fluid for increasing the efficiency of the solar collector, and the concept of nanofluid has emerged. In 1995, Choi and Eastman mentioned that low thermal conductivity was the main limitation in the development of a working fluid. They conceived the innovative idea of adding metallic nanoparticles (copper nanophase material) to the heat transfer fluid to enhance the fluid's thermal conductivity [8]. Later, more researchers started investigating this new concept, which was a major breakthrough for heat transfer. On January 22, 2020, while searching for papers published after 2019 with the keyword "Nanofluid Enhanced Heat Properties" on Google Scholars, and 11,900 results came out. This number is impressive and it shows that many researchers are pursuing research in this concept. In Kaggwa and Carson's review [9], it was pointed out that the thermal conductivity of some solids is higher than that of convectional heat transfer fluids, such as water, oil, and ethylene glycol. The addition of the stable nanoparticles can enhance the thermal conductivity of the heat transfer fluid. Xuan and Li's study in 2000 [10] found that the addition of nanoparticles to the heat transfer fluid can increase the surface area and the thermal properties of the fluid, such as heat capacity (Cp) and thermal conductivity (K).

Several types of nanoparticles have been used in recent studies. One type comprises single elements, such as copper, aluminum, and silicon; and another type consists of single element oxide such as CuO, Al_2O_3, and TiO_2.

Nanofluids can be of two types: single material nanofluids and hybrid nanofluids. The former contains only one type of nanoparticles, such as Cu-water base or CuO-water

base, whereas the latter comprises more than one type of nanoparticles, such as CNT-Cu/H_2O or CNT-Au/H_2O (CNT denotes “carbon nanotube”) [11].

A survey on Google Scholar showed that two types of nanofluids have been frequently used in recent research, namely, CuO and Al_2O_3. There are 3140 results for “CuO nanofluid enhancement” and 3090 results for “Al_2O_3 nanofluid enhancement” after 2019. Most of the researchers have successfully used these two types of nanoparticles with multiple types of base heat transfer fluids to achieve the high heat transfer compared with the heat transfer provided by conventional working fluids.

All these studies have shown that nanofluids can facilitate high heat transfer. Chaudhari *et al.* [12] used different volume fractions of Al_2O_3 and CuO nanofluids for heat transfer application and showed that when the volume fraction of Al_2O_3 and CuO was between 0.05% and 1%, the thermal conductivity ratio increased noticeable. Phor et al. [13] synthesized Al_2O_3-water nanofluid and designed a self-cooling device that operated without any external power input. They examined the effect of Al_2O_3 nanofluids with different volume fractions on the rate of transfer the heat load to the heat sink. Their results showed that the heat load was apparently cooled by 15℃, 13℃, and 12℃ at volume fractions of 1.5%, 1%, and 0.5%, respectively. Rafi et al. [14] combined each of two different water-EG mixtures with different proportions of the two constituents with various volume fractions of Al_2O_3 and CuO and examined their use as cooling fluid in radiators. They observed that the heat transfer potential of nanofluid increased. Venkitaraj and Suresh [15] examined the combination of PE with 0.1 wt% of Al_2O_3, CuO, and TiO_2 nanoparticles for 500 thermal cycles by using thermogravimetry-differential thermogravimetric analysis, differential scanning calorimetry, and Fourier

transform infrared. The addition of nanoparticles caused an apparent decrease in the heat flow rate. After 500 thermal cycles, the enthalpy of the solid-solid transition of PE containing nanoparticles decreased compared with that of pure PE. Sivasubramanian et al. [16] examined the use of an aluminum minichannel for computer microprocessor cooling for CuO-water nanofluid (24nm) with 0.1% and 0.5% volume fraction, and found that the CuO-water nanofluid enhance the performance as the working fluid. Zheng et al. [17] examined the effects of Al_2O_3-water nanofluid with different volume fractions on the heat transfer performance of a counter-flow double-pipe exchanger. The results showed that if the volume fraction of the nanoparticles increased, the Nusselt number improved while the Reynolds number decreased. Sulgani and Karimipour [18] examined the effect of an Al_2O_3-Fe_2O_3 nanopowder hybrid on 10w40 engine oil, and their results showed that the addition of even a small mass concentration improved the thermal properties of the engine oil. Yu et al. [19] found that adding graphene nanosheets to ethylene glycol increased the thermal conductivity of a latter. Gupta et al. [20] examined the heat transfer performance of graphene nanofluid. They noted that the thermal conductivity increased noticeably even for a low volume concentration. The above-mentioned studies helped improve the understanding of how the innovative idea of Choi and Eastman [8] could influence research in the future, and how nanofluid can enhance the ratio of heat transfer.

1.4 Solar Energy's Optimizing Method

Performance improvement in solar energy systems is the priority goal that needs to be solved. In 2019, the solar panels produced by SunPower had the highest efficiency up to 22.8% [21]. Researchers have used various approaches to enhance the performance of solar energy systems. Kumar et al. [22] modified the heat-absorbing side of a solar air

heater (SAH) with ribs; their results showed that the heat transfer improved noticeably. Liu et al. [23] found that the use of SnO_2 as the electron transport layer (ETL) in perovskite solar cells resulted in excellent transmission with an appropriate energy bandgap, a deep conduction band level, and high electron mobility. SnO_2 is one of the most promising materials for use as the ETL. Rezaei et al. [24] observed that the use of a combination of carbon dots (CDs) and TiO2 can enhance a dye-sensitized solar cell's (DSSC) power conversion efficiency compared with the use of pure TiO2. Jian et al. [25] found that Cs-doped Sb2S3 is the most effective enhancement between (Li, Na, K, Rb, Cs), which improves the solar cell performance. Ebrahimi et al. [26] examined the doping of the mesoscopic TiO_2 ETL of a solar cell with different amounts of graphene quantum dots (GDQs), and they observed a significant improvement in the solar cell's performance.

1.5 Use of nanofluids in the field of Solar Energy

Since the work of Choi and Eastman [8], many studies have used nanofluids for solar energy research. Sarafraz et al. [27] used acetone containing carbon nanoparticles as the nanofluid to enhance the thermal performance of evacuated tube solar thermal collectors. Nazari et al. [28] examined the performance of Cu_2O nanofluid in a single slope solar still with a thermoelectric glass cover cooling channel. Sözen et al. [29] used TiO_2-deionized water as a working fluid to enhance the heat transfer rate in a plate heat exchanger. Malekan et al. [30] used Fe_3O_4/Therminol 66 and CuO/Therminol 66 as the working fluids under an external magnetic field for a parabolic trough solar collector (PTSC). They noted that reducing the size of nanoparticles or enhancing the nanoparticle volume concentration increased the coefficient of convective heat transfer, Nusselt

number, performance evaluation criteria, and efficiency of the PTSC. Vakili et al. [31] examined the use of graphene nanoplatelets/deionized water in a laboratory sample of a volumetric collector and found that the efficiency of the solar collector increased with the weight fraction of the nanofluid. Iranmanesh et al. [32] used graphene nanoplatelets/distilled water nanofluid as the absorption medium in an evacuated tube solar collector, and they observed that the solar collector's efficiency showed noticeable enhancement with an increase in the mass percentage of nanoparticles. Sharafeldin et al. [33] examined the effect of the volume fraction of Cu-water nanofluid on the absorbed energy. Bellos et al. [34] examined the use of various nanoparticles with thermal oil (Syltherm 800) as the working fluid in PTSCs, and their results showed that a higher concentration of nanoparticles could enhance the performance of the collectors. Dehaj and Mohiabadi [35] examined the use of MgO-water nanofluid with different volume fractions as the working fluid in an evacuated heat pipe solar collector (HPSC). The performance of the HPSC showed obvious enhancement with increasing concentration of the MgO-water nanofluid.

1.6 Motivation

This study was aimed at understanding how the volume fractions of the nanofluid and type of nanoparticles in the nanofluid could influence the performance of flat plate collectors. The study was based on a simulation employing a computational fluid dynamics method in COMSOL Multiphysics.

The effects of two working fluids, namely, water and water-based nanofluid, on the heat transfer of an FPSC were compared.

The volume concentration of Al_2O_3 and CuO nanoparticles affected the nanofluid properties such as density, viscosity, heat capacity, and thermal conductivity and the property changes influenced the performance of the FPSC. The parameters of the FPSC considered in this study were the outlet temperature, efficiency, and pressure drop.

Chapter II

Flat Plate Solar Collector Model

Many types of solar collectors were introduced in the preceding chapter. This chapter discusses the design of the flat plate solar collector. The model used in the simulation is introduced and details of the model, including its geometry, parameters, and the materials of the FPSC, are provided.

2.1 Flat Plate Solar Collector

The flat plate solar collector is probably the most commonly and widely used solar collector [36]. It consists of an absorber (which is mostly copper), pipes attached to the absorber, and an external case, which is usually an insulation box with a transparent glass cover through which solar radiation can pass to the absorber [37]. There are typically two horizontal pipes at the top and at the bottom, which are called headers, and several small vertical pipes called risers [38]. The principle of the flat plate solar collector is that energy is collected by the absorber when solar radiation is incident on it through the glass cover. The working fluid, such as water, emerges from the collector's bottom header, passes through the risers, collects the heat from the absorber plate, and exits through the top header [38]. Figure 1 (taken from [39]) shows a three-dimensional model of a flat plate collector, it shows the detailed structure of a flat plate collector.

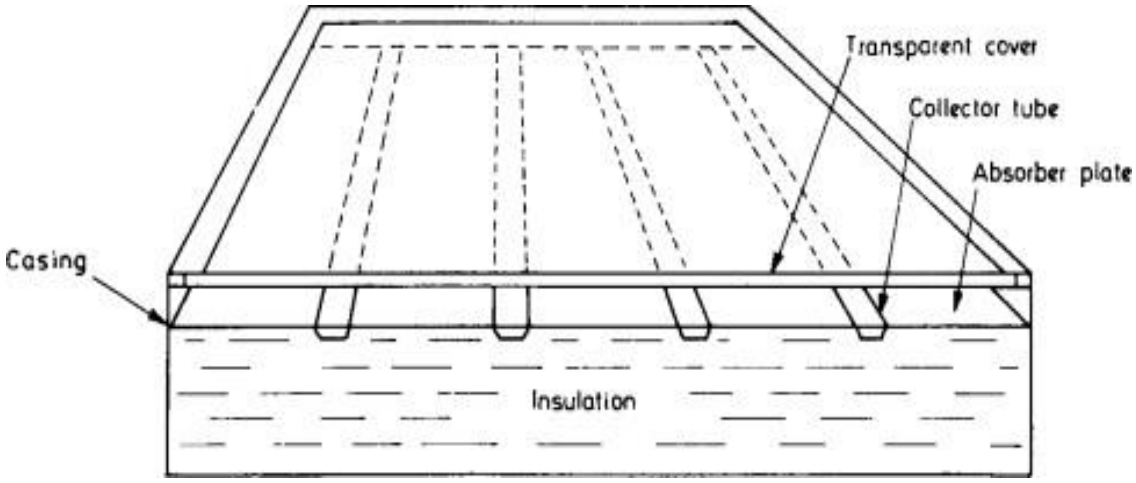

Figure 1. Three-dimensional model of a flat plate collector [39]

A solar water heating system contains a flat plate solar collector. There are two types of solar water heating systems: direct hot water systems and indirect hot water systems. The only difference between them is that the latter contains a heat exchanger, which can make the flat plate solar collector more efficient [40]. Figures 2 and 3 (taken from [40]) shows the structures of the two types of solar water heating systems.

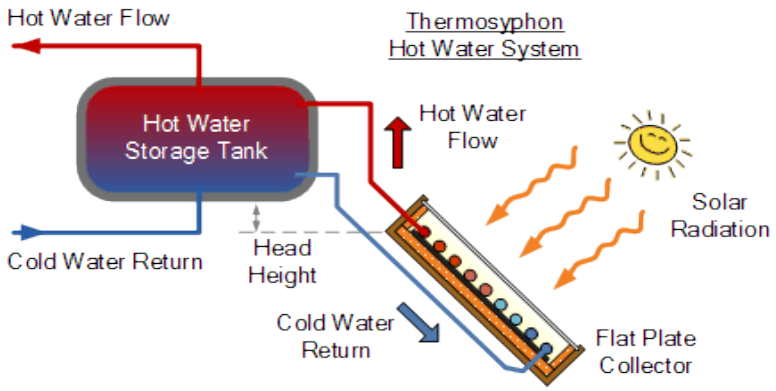

Figure 2. Direct hot water system [40]

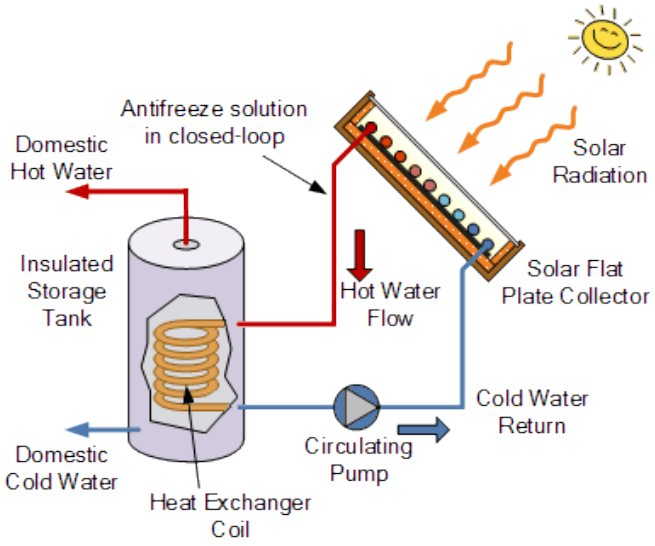

Figure 3. Indirect hot water system [40]

2.2 Use of Nanofluid in Flat Plate Solar Collector

It is of interest to examine how replacing water with nanofluid can improve the heat transfer performance of a flat plate solar collector (FPSC). Jouybari et al. [41] used SiO_2/deionized water as the working fluid to enhance the thermal performance of an FPSC. Saffarian et al. [42] examined the use of Al_2O_3-water and CuO-water nanofluids with different volume fractions. In an FPSC, the nanofluid passes through U-shaped, wavy, spiral pipes with identical lengths. Using a wavy tube and 4% CuO-water nanofluid can significantly increase the heat transfer coefficient. Stalin et al. [43] examined the use of low concentration CeO_2-water and water as the working fluids in an FPSC and found that CeO_2-water could enhance the performance of the FPSC. Arora et al. [44] compared the use of Al_2O_3/water and pure water in a Marquise shaped channel FPSC, in which there were two aluminum absorber plates sandwiched together. They found that the nanofluid improved the efficiency of the flat plate collector. Akram et al. [45] examined the effect of clove-treated graphene nanoplatelet nanofluids on FPSCs.

They used different mass concentrations and mass flow rates in their experiments, and the results showed that increasing the mass concentration of the nanofluid and increasing the mass flow rate could enhance the thermal performance of a flat plate collector.

2.3 Geometry

The two-dimensional FPSC model chosen in this study was adopted from Nasrin and Alim's paper [46]. Figure 4 shows a schematic of the FPSC used by that Nasrin and Alim.

Figure 5 shows the two-dimensional model used in the simulation of the current study. The model comprises of a transparent glass cover, a high-thermal-conductivity copper absorber plat, a copper rising pipe, an air gap, and an external wooden box. The model has been sketched by using the geometry function of COMSOL Multiphysics, and the parameters and specific boundary conditions are described later.

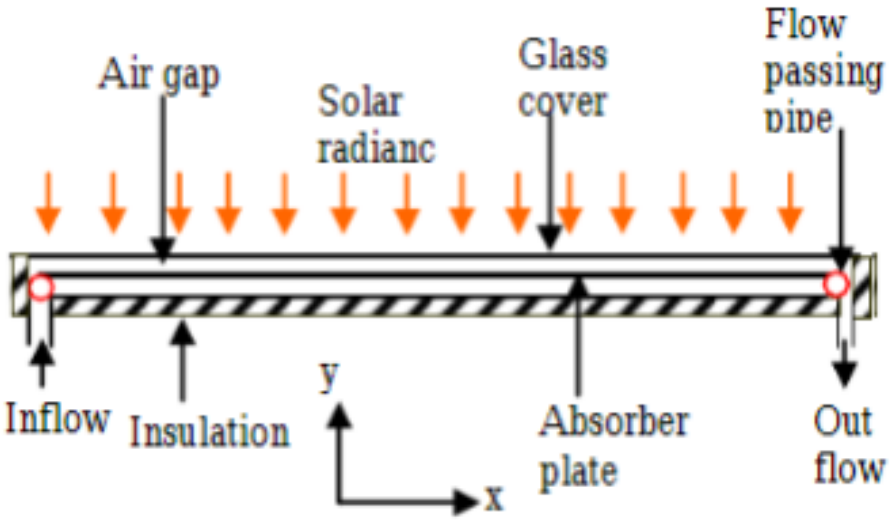

Figure 4. Schematic of an FPSC [46]

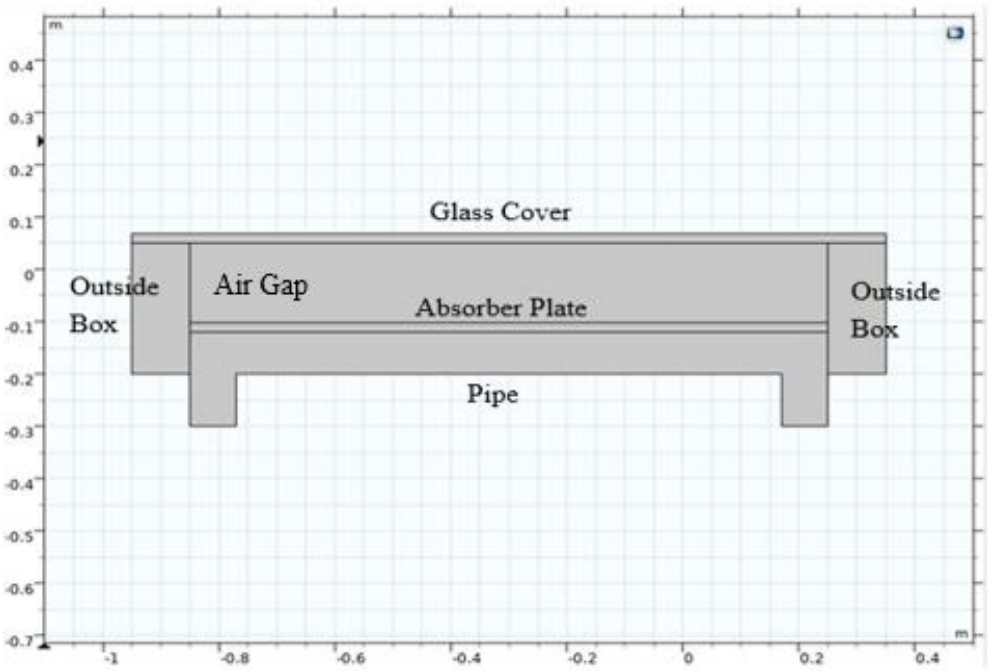

Figure 5. Two-dimensional FPSC model used in the present study

The solar radiation passes through the glass cover and is absorbed by the absorber plate. The working fluid in the pipe absorbs heat from the absorber plate. The main objective of this study was to investigate the temperature rise of the working fluid after it absorbs solar heat and exits from the outlet. Table 1 lists the parameters used in the Two-dimensional FPSC model.

Parameter	Material	Area (m^2)
Cover	Glass	1.3 (L) × 0.018 (W)
Absorber Plate	Copper	1.1 (L) × 0.018 (W)
Outside Box	Wood	Left Side: 0.1 (L) × 0.25 (W) Right Side: 0.1(L) × 0.25 (W)
Gap	Air	1.1 (L) × 0.152 (W)
Pipe	Copper	0.08 (D) × 1.3 (L)

Table 1. Parameters of FPSC

Chapter III

Mathematical Modeling

In the present study, the heat transfer from the absorber to working fluid was investigated by considering the working fluid to have steady-state laminar flow. The mathematical details, such as the governing equations and equations describing the nanofluid heat properties, is outlined in this chapter. Simulations were performed on COMSOL Multiphysics.

3.1 Governing Equations for Single-Phase Fluid Flow

A working fluid to which solid nanoparticles have been added is generally considered as a two-phase fluid; however, in some conditions, the nanofluid can be assumed as a homogeneous single-phase fluid [47] since the nanoparticles are minute (<100 nm) and easily fluidized [48]. Under the assumption that there is no slip between phases and that the phases are in thermal equilibrium, the governing equations for incompressible laminar flow and heat transfer are presented below.

In the simulation, forced convection rather than natural convection was assumed, and the fluid flow was considered to be incompressible. In forced convection, gravity is considered as the body force inside the tube [49].

3.1.1 Continuity Equation

$$\frac{\partial}{\partial x_j}\left(\rho_{nf} u_j\right) = 0 \tag{1}$$

Here, u and ρ_{nf} are the fluid velocity and density of the nanofluid, respectively.

In COMSOL, the continuity equation is presented as

$$\rho \nabla \cdot (\mathbf{u}) = 0 \tag{2}$$

where *u* and ρ are the velocity and density of the nanofluid, respectively.

3.1.2 Momentum Equation

$$\rho_{nf}\left(\frac{\partial u_i u_j}{\partial x_j}\right) = -\frac{\partial P}{\partial x_i} + \frac{\partial}{\partial x_j}\left(\mu_{nf}\frac{\partial u_i}{\partial x_j}\right) \tag{3}$$

Here, *P* and μ_{nf} are the pressure and viscosity of the nanofluid, respectively.

In COMSOL Multiphysics, the momentum equation is presented as

$$\rho(\mathbf{u} \cdot \nabla)\mathbf{u} = \nabla \cdot [-p\mathbf{I} + \mathbf{K}] + \mathbf{F} + \left(\rho - \rho_{ref}\right)\mathbf{g} \tag{4}$$

$$\mathbf{K} = \mu(\nabla \mathbf{u} + (\nabla \mathbf{u})^{\mathrm{T}}) \tag{5}$$

where p denotes the pressure; *F*, the volume force; *u*, the velocity; ρ, the density; and *g*, the gravity.

3.1.3 Energy Equation

$$\frac{\partial}{\partial x_j}\left(u_j T\right) = \frac{k_{nf}}{\rho_{nf} C p_{nf}}\left(\frac{\partial^2 T}{\partial x^2{}_j}\right) \tag{6}$$

Here, Cp_{nf} and k_{nf} are the specific heat and thermal conductivity of the nanofluid, respectively, and *T* denotes the temperature.

In COMSOL Multiphysics, the energy equation is presented as

$$d_z \rho C_P \mathbf{u} \cdot \nabla T + \nabla \cdot \mathbf{q} = d_z Q + q_0 \tag{7}$$

$$\mathbf{q} = -d_z k \nabla T \tag{8}$$

3.2 Physical Properties of Water and Water-Based Nanofluid

The addition of nanoparticles influences the physical properties of a fluid, such as the density, specific heat, thermal conductivity, and dynamic viscosity. In this section, the calculation of the thermophysical properties of the nanofluid is explained. Unless otherwise stated, the equations are based on the two-component mixture rule [50].

3.2.1 Density of Nanofluid

The density of the nanofluid was calculated from the two-component mixture rule.

$$\rho_{nf} = (1 - \emptyset)\rho_{bf} + \emptyset \rho_p \tag{9}$$

Where ρ_{bf} is the density of the base fluid, ρ_p is the density of the nanoparticles, and $\emptyset$ is the volume concentration of nanoparticles.

3.2.2 Specific Heat of Nanofluid

The two-component mixture rule can be applied to predict the properties of the nanofluid, and the deviation between experimental and theoretical values can be considered as the 10% error [51].

$$C_{P,nf} = \frac{(1-\emptyset)\rho_{bf}C_{P,bf}+\emptyset\rho_p C_{P,p}}{(1-\emptyset)\rho_{bf}+\emptyset\rho_p} \quad (10)$$

Here, $C_{P,p}$ is the specific heat of the nanoparticles and $C_{P,bf}$ is the specific heat of the base fluid.

3.2.3 Thermal Conductivity of Nanofluid

The thermal conductivity of the nanofluid can be calculated at all the evacuated temperatures by using the Maxwell equation, and the maximum error in the calculation is 1.18% [51].

$$k_{nf} = \frac{k_p+2k_{bf}+(k_p-k_{bf})\emptyset}{k_p+2k_{bf}-(k_p-k_{bf})\emptyset}k_{bf} \quad (11)$$

Where k_p is the thermal conductivity of the nanoparticles and k_{bf} is the thermal conductivity of the base fluid.

3.2.4 Viscosity of Nanofluid

There are many theoretical models for determining the viscosity. One of the famous models was published by Einstein in 1906 [52]. The Einstein model is valid for low volume concentrations ($\emptyset$<0.02) [53]. However, since high volume concentrations

were to be considered in the simulation in the present study, the model of Kitano et al. [54] was used.

$$\mu_{nf} = \mu_{bf}(1 - \frac{\emptyset}{\emptyset_m})^{-2} \quad (12)$$

$$\emptyset_m = 5.10^{-6}T^2 - 4.10^{-4}T + 0.118 \quad (13)$$

Where μ_{bf} is the viscosity of the base fluid, $\emptyset$ is the volume concentration of the nanofluid, and $\emptyset_m$ is the maximum packing fraction that the nanoparticles can achieve [51].

Tables 2 and 3 list the physical properties of materials and the associated nanofluids with different volume concentrations, respectively.

Material	$\boldsymbol{k}\ (\boldsymbol{W \cdot m^{-1} \cdot K^{-1}})$	$\boldsymbol{c_P}\ (\boldsymbol{J \cdot kg^{-1} \cdot K^{-1}})$	$\boldsymbol{\mu}\ (\boldsymbol{Pa \cdot s})$	$\boldsymbol{\rho}\ (\boldsymbol{kg \cdot m^{-3}})$
Water	0.576	4180	0.0008891	1000
Al_2O_3	40	765	-	3970
CuO	18	540	-	6510

Table 2. Physical properties of materials [55, 56]

Nanofluid	$k\ (W \cdot m^{-1} \cdot K^{-1})$	$c_P\ (J \cdot kg^{-1} \cdot K^{-1})$	$\mu\ (Pa \cdot s)$	$\rho\ (kg \cdot m^{-3})$
Al_2O_3 0.5%	0.5843	4113.2	0.0010443	1014.85
Al_2O_3 1%	0.5927	4048.33	0.0012427	1029.7
CuO 0.5%	0.5839	4064.69	0.0010443	1027.55
CuO 1%	0.5919	3955.41	0.0012427	1055.1

Table 3. Physical properties of nanofluid

Two types of nanoparticles were chosen for use in the simulation, namely, Al_2O_3 and CuO, and two different volume concentrations (0.5% and 1%) were also chosen for comparison purposes.

3.3 Pressure Drop and Pumping Power of Nanofluid

The forced convection in the flat plate solar collector (FPSC) pipe required a mechanical pump to push it [57]. The inlet and outlet pressures were measured in COMSOL, and the pressure difference between them was the pressure drop.

The following equation was used to relate the pressure drop to the calculated pumping power.

$$\text{Pumping power } = \left(\frac{\dot{m}}{\rho}\right) \text{ x } \Delta P = \Delta P \text{ x } V = \frac{\rho.g.V.h}{\eta_p} \tag{14}$$

Where $\dot{m}$ is the mass flow rate, ρ is the density, ΔP is the pressure drop, V is the volume flow rate, g is the gravity, h is the differential height, and η_p is the pump efficiency.

3.4 Efficiency of FPSC

Q is the amount of solar radiation received by the FPSC. In this study, a constant heat flux was set to be the heat source of the solar collector.

$$Q_{rec} = q''A \tag{15}$$

Here, q'' is the constant solar heat flux and *A* is the surface area of the absorber plate.

The working fluid in the tube extracts some heat when it flows through the absorber plate:

$$Q_{abs} = \dot{m} \times C_P \times (T_{out} - T_{in}) \tag{16}$$

The following equation can calculate the efficiency η of the solar collectors:

$$\eta = \frac{\dot{m} \times C_P \times (T_{out} - T_{in})}{q''A} \tag{17}$$

3.5 Boundary Conditions

The boundary conditions comprised inlet, outlet, wall, constant pressure, axisymmetric, symmetric, and periodic conditions [58]. In COMSOL, conjugate heat transfer, which includes the solid and fluid heat transfer, and laminar flow were considered in the simulation model. Figure 6 shows the function interface in COMSOL.

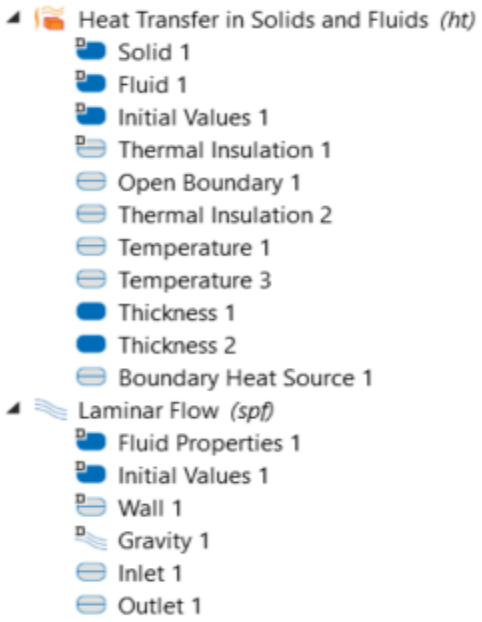

Figure 6. Conjugate heat transfer function interface in COMSOL

3.5.1 Inlet

In this boundary condition, the flow rate or velocity of the fluid is defined. In the simulation, the density of the nanofluid varied with the temperature, and this would have rendered the results temperature dependent. Therefore, in the simulation, the mass flow rate was used instead of the volume flow rate. Figure 7 shows how the inlet was defined in the model.

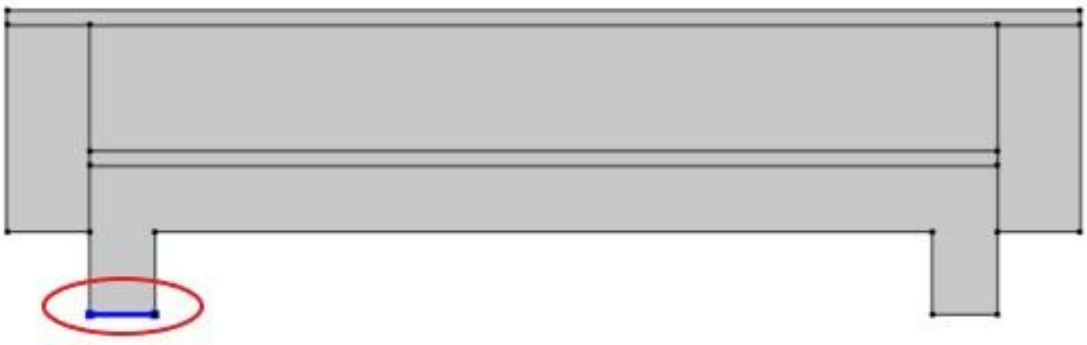

Figure 7. Inlet of FPSC

For the inlet boundary condition, the mass flow rate was 0.004 kg/s, and the default channel thickness was d_{bc} = 1 m.

In COMSOL, the equation for the inlet boundary condition is as follows:

$$-\int_{\partial\Omega}\rho(\mathbf{u}\cdot\mathbf{n})\mathrm{d_{bc}}\,dS=\dot{m} \tag{18}$$

where ρ is the density, d_{bc} is the channel thickness, $\boldsymbol{u}$ is the velocity, S is the surface area, and $\dot{m}$ is the mass flow rate.

The temperature of the inlet was uniform. In the simulation, the inlet temperature was set to 298 K.

3.5.2 Outlet

The opposite side of the pipe was defined as the outlet, and it was the part from where the working fluid flowed out. The mass flow rate of the working fluid was constant, and therefore, the mass flow rate of the outlet was also 0.004kg/s. Figure 8 shows the position of the outlet in the simulation, and Figure 9 shows the velocity field in the simulation.

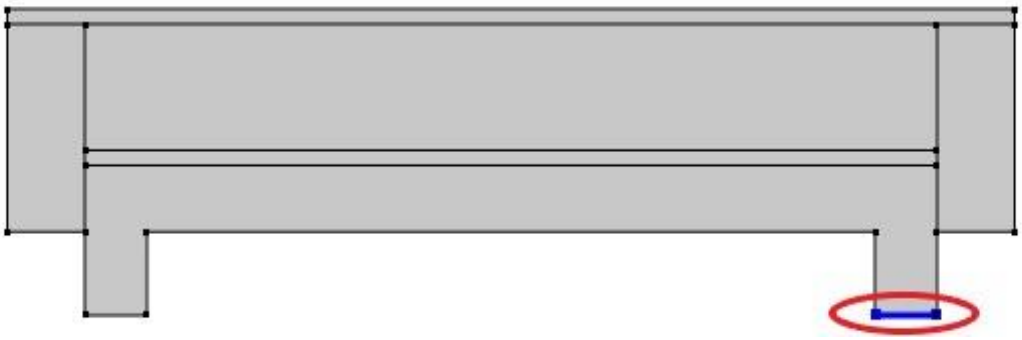

Figure 8. Outlet of FPSC

Figure 9. Velocity field in FPSC

In the outlet boundary, the pressure P_0 is set to 0 Pa. The pressure here is the relative pressure, not the absolute pressure.

In COMSOL, the equation for the outlet boundary condition is

$$[-p\mathbf{I} + \mathbf{K}]\mathbf{n} = -\widehat{\boldsymbol{p_0}}\mathbf{n} \tag{19}$$

$$\widehat{p_0} < p_0 \tag{20}$$

3.5.3 Thermal Insulation

In the simulation, several boundary conditions included thermal insulation, implying that the conditions were not affected by the convection or the heat source. Figure 10 shows the thermal insulation boundary condition set in the model.

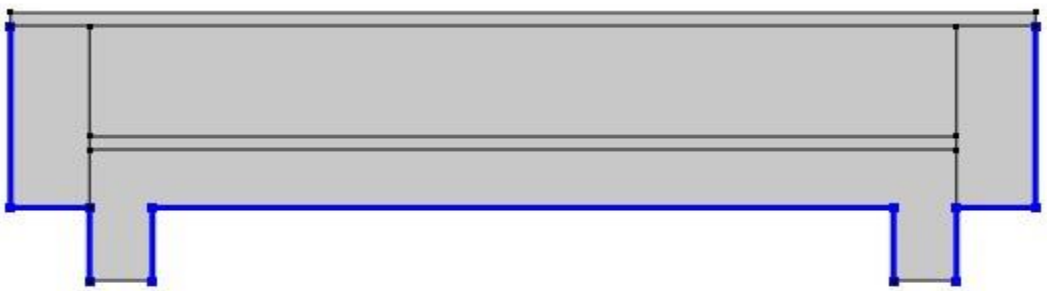

Figure 10. Thermal Insulation

The equation used for thermal insulation in COMSOL

$$-\mathbf{n} \cdot \mathbf{q} = 0 \tag{21}$$

3.5.4 Heat Source

In an FPSC, the heat source provides a constant heat flux to the tube. In the model, the heat source is located at the absorber plate. Figure 11 shows the area defined as the heat source. The general heat source is 800 W/m^2

The equation for the heat source in COMSOL is

$$-\mathbf{n} \cdot \mathbf{q} = d_z Q_b \tag{22}$$

where Q_b is the general heat source, and d_z is the thickness in the *z*-direction (COMSOL's default is 1).

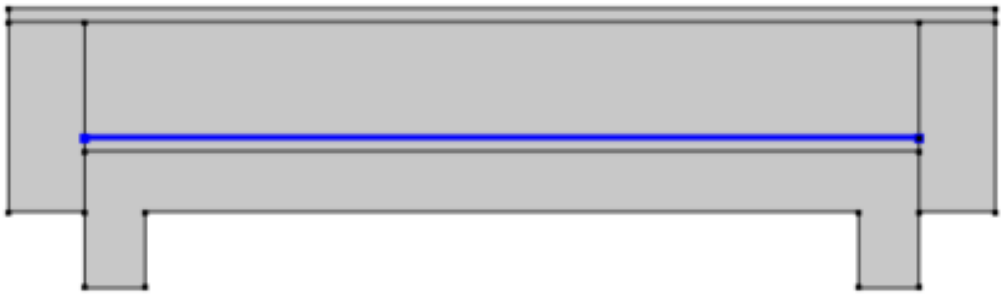

Figure 11. Heat source of FPSC

3.5.5 Temperature

Figure 12 shows the region with the ambient temperature; it is at the top of the glass cover. The ambient temperature was set to 298 K.

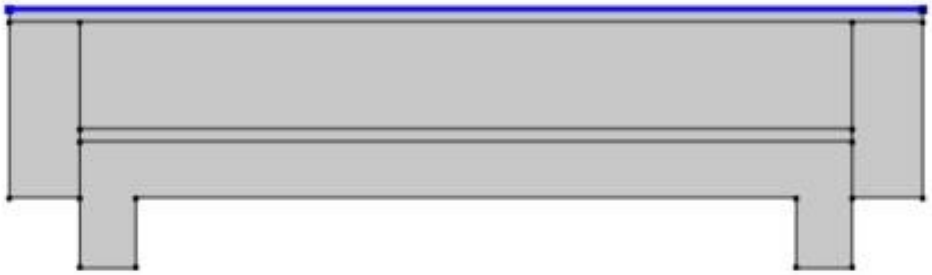

Figure 12. Ambient temperature at the top of the glass cover

3.6 Computational Mesh

The mesh is one of the key factors in Computational fluid dynamics. The quality of the grid can determine the rate of convergence, the accuracy of the solution, and the required CPU time [59]. There is a function in COMSOL, called “Physics-controlled mesh,” that automatically generates a mesh. For the element size “fine,” there are 8480 domain elements and 707 boundary elements, the element size has better performance and provides a more accurate result than “normal” (5693 domain elements and 575 boundary elements), however, the required CPU time is longer. Figures 13 and 14 show meshes with “normal” element size and “fine” element size.

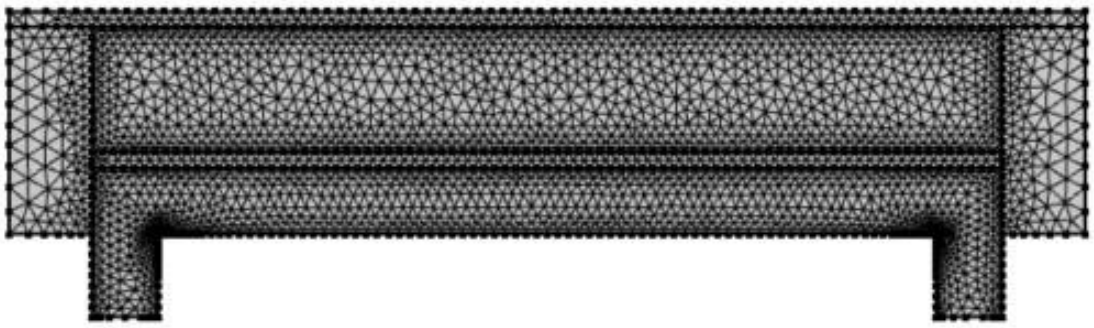

Figure 13. Mesh with “normal” element size

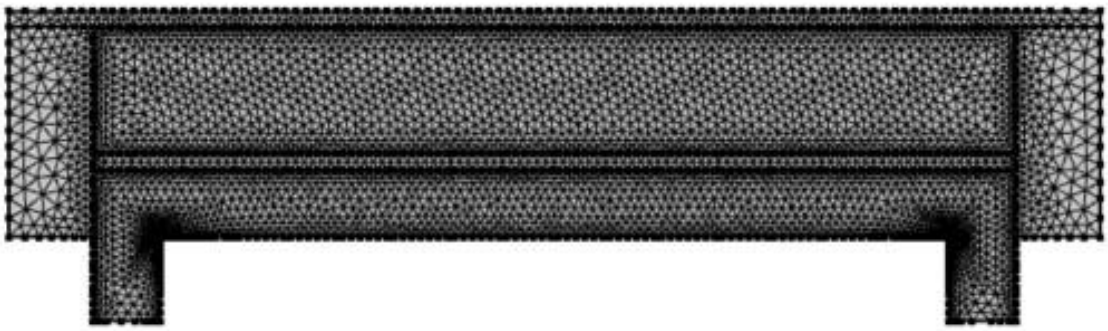

Figure 14. Mesh with “fine” element size

Chapter IV

Results and Discussion

This chapter mainly discusses the simulation results, including those pertaining to the outlet temperature of the fluid, efficiency of the solar collector, and the pressure drop.

4.1 Outlet Temperature

Five different working fluids were considered in this study - water, 0.5% Al_2O_3/water, 1% Al_2O_3/water, 0.5% CuO/water, and 1% CuO/water. By using material sweep in COMSOL, the results for these five working fluids could be computed simultaneously, which made the comparison of the results easier. Adding nanoparticles to the base fluid changed the thermo physical properties of the fluid, resulting in a change in the simulation results. In this study, the inlet temperature of the fluid was set to 298 K. A working fluid with nanoparticles has a higher outlet temperature, and a higher volume concentration of nanoparticles also leads to a higher outlet temperature. Figure 15 shows the result of the simulation for the outlet temperature, which agrees with the statement above; Figures 16 and 17 show that the addition of nanoparticles significantly affected the simulation result.

The results also indicate that the CuO nanoparticles showed better performance than the Al_2O_3 nanoparticles because of the difference in their thermo physical properties. CuO nanofluid has a smaller specific heat C_P than Al_2O_3 nanofluid, which

explains why the outlet temperature of the CuO nanofluid was higher than that of Al_2O_3 nanofluid.

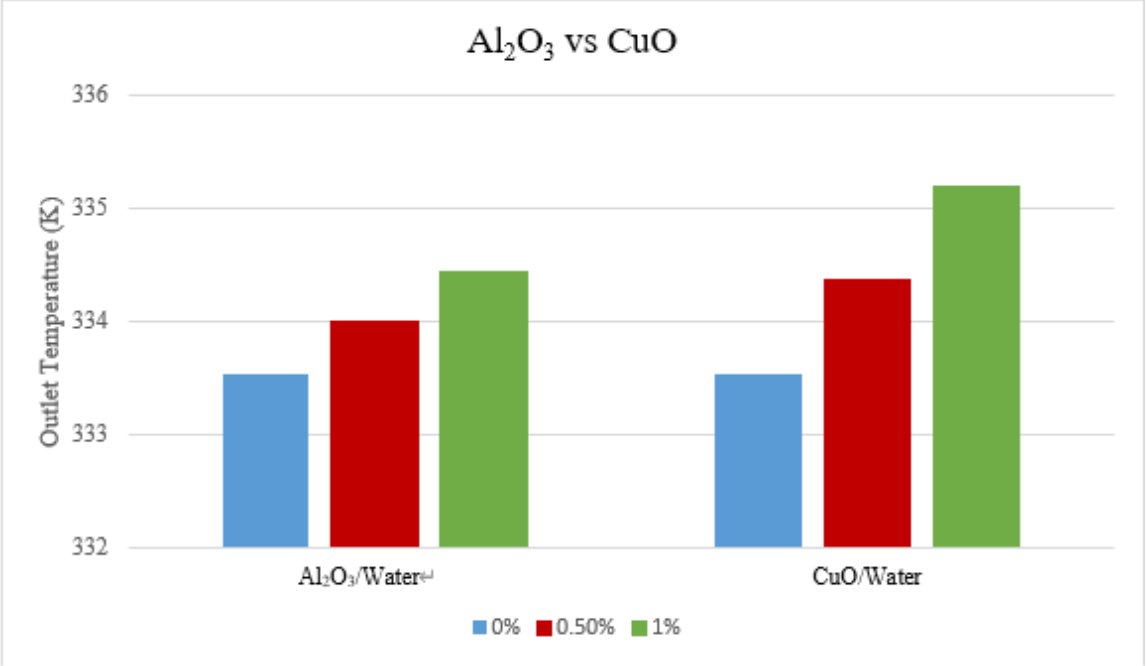

Figure 15. Comparison of outlet temperature between Al_2O_3 and CuO

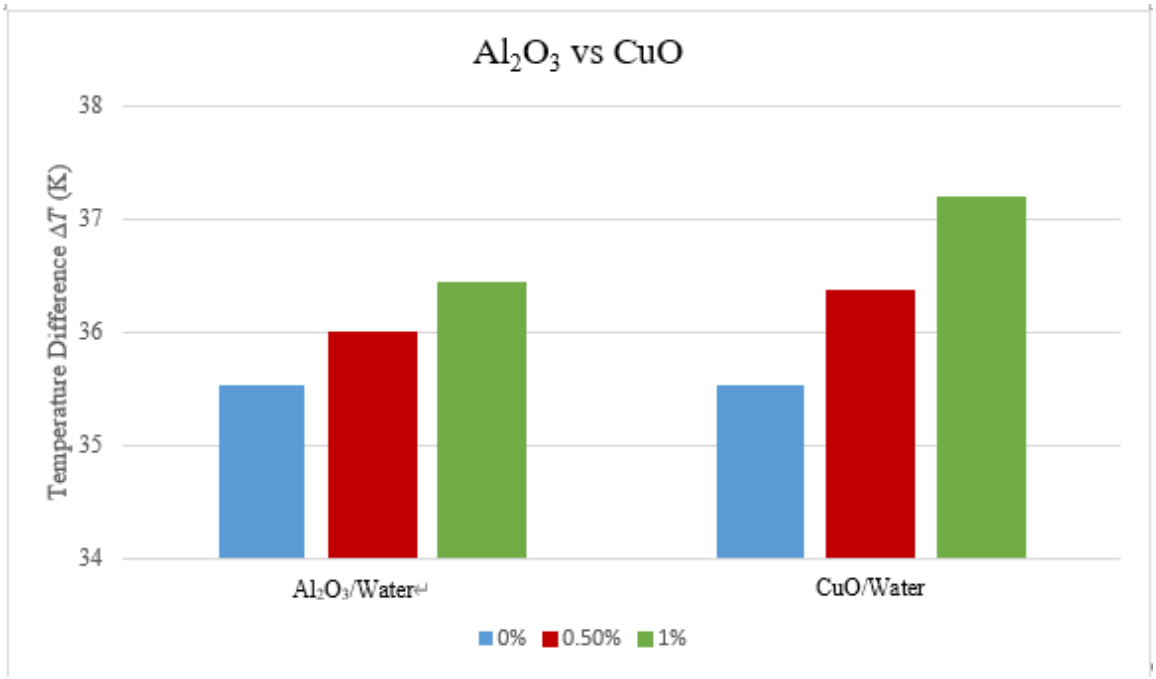

Figure 16. Comparison of temperature difference between Al_2O_3 and CuO ΔT

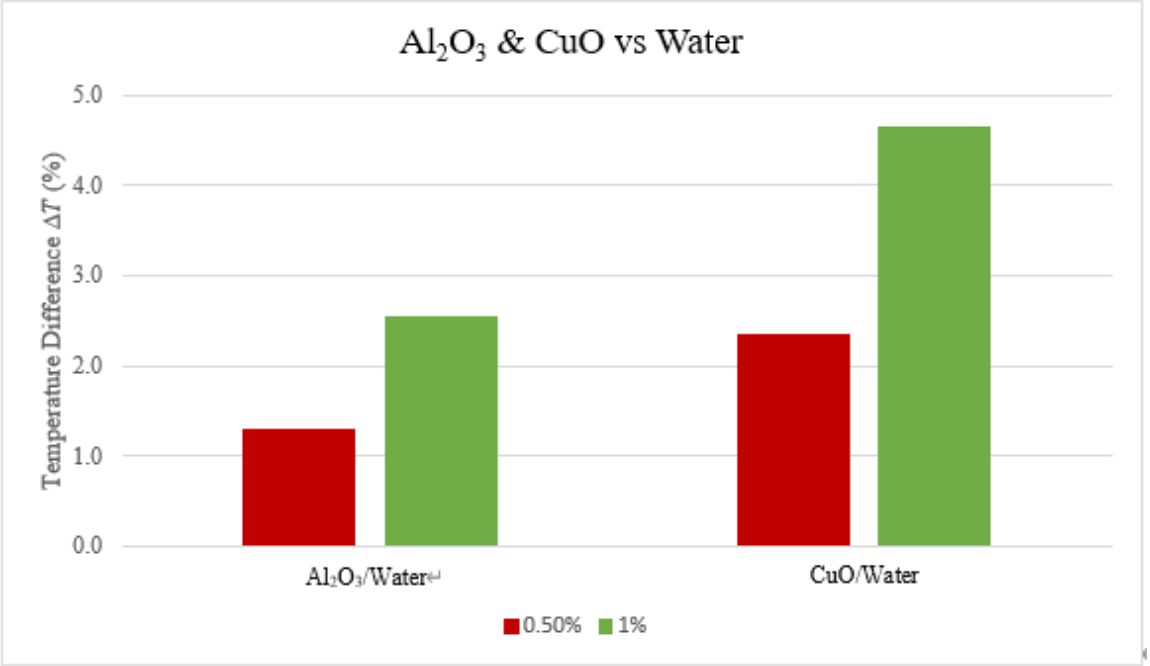

Figure 17. Comparison of temperature difference % between Al_2O_3/CuO nanofluid and water

Figures 18 and 19 show the temperature distributions for different volume concentrations of the nanofluids in water.

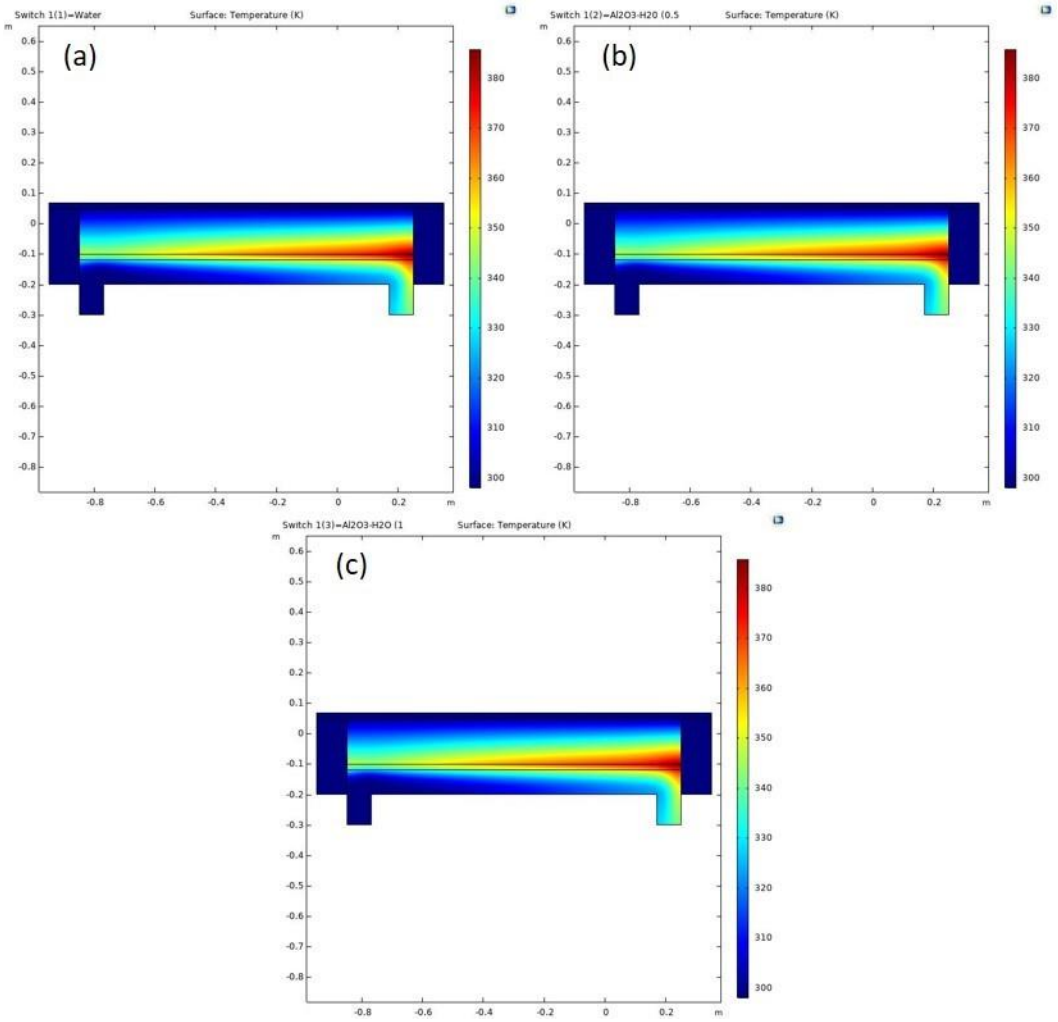

Figure 18. Temperature distribution of Al_2O_3/water for volume concentrations of (a) 0%, (b) 0.5%, and (c) 1%

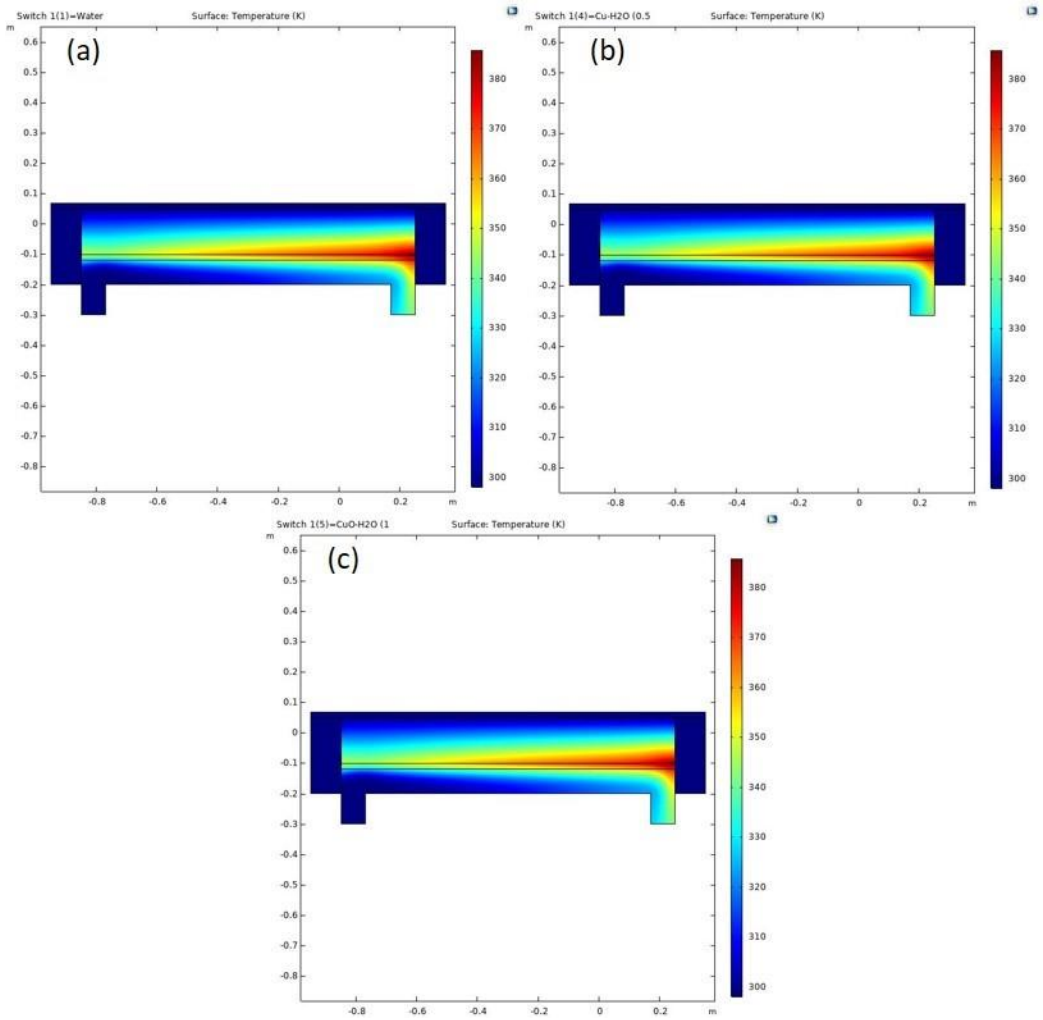

Figure 19. Temperature distribution of CuO/water for volume concentrations of (a) 0%, (b) 0.5%, and (c) 1%

4.2 Efficiency of flat plate solar collector

Efficiency is one of the critical indexes to evaluate the performance of solar collectors. Several papers have pointed out that the addition of nanoparticles enhances the efficiency of solar collectors. Apart from the results of the simulation, results from previous studies are also discussed in this session.

In the simulation, five different materials were used as the working fluid to test the efficiency of the FPSC, namely, water, 0.5% Al_2O_3, 1% Al_2O_3, 0.5% CuO, and 1% CuO. After the calculations, the results obtained were quite different from those of other studies. For a mass flow rate of 0.004 kg/s, the efficiency was 69.59% for water; 69.36% and 69.11% for 0.5% and 1% of Al_2O_3, respectively; and 69.28% and 68.94% for 0.5% and 1% of CuO, respectively. Evidently, the addition of nanoparticles decreased the efficiency. The reason for this is that the nanoparticles' absorption rate and reflection rate were not considered in the simulation. Even though the outlet temperature has significantly increased following the addition of nanoparticles. Another reason could be that the design of the model limited the heat transfer, and the energy dissipated through natural convection was not considered.

In the simulation, parametric sweep was used to evaluate the effect of different mass flow rates; the parametric sweep included the values 0.004, 0.008, 0.012, 0.024, and 0.048 kg/s. An increase in the mass flow rate resulted in a significant increase in the efficiency of the flat plate solar collectors (FPSCs). Figures 20 and 21 depict the charts of the efficiency of FPSCs with Al_2O_3/water and CuO/water as the working fluids; the trend in the charts express the results of the efficiency in FPSCs.

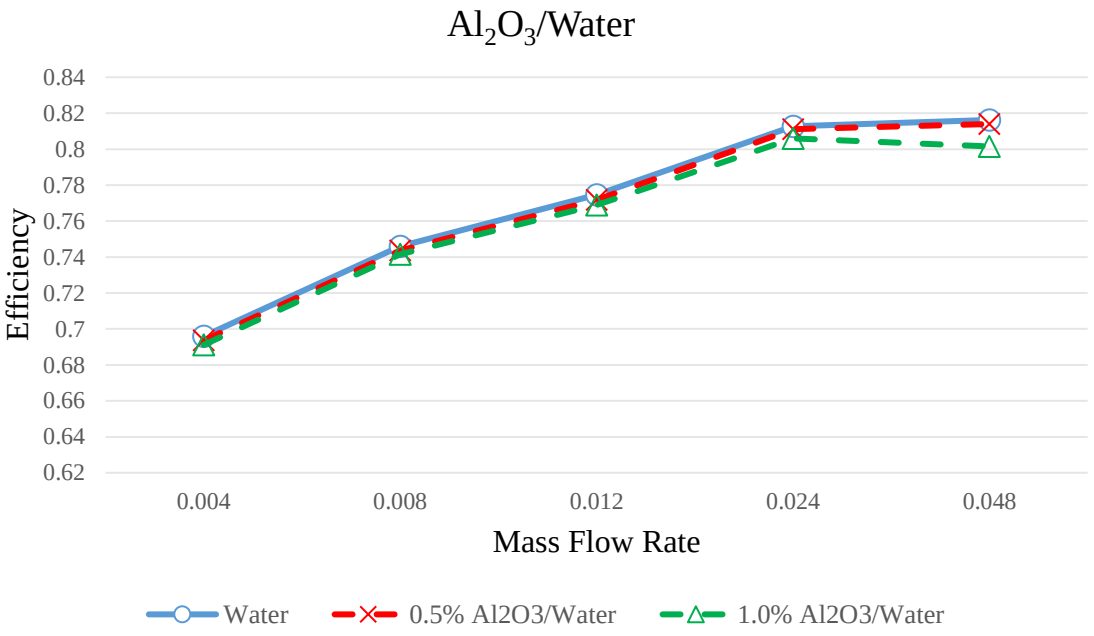

Figure 20. Efficiency of the FPSC when Al_2O_3/Water as the working fluid

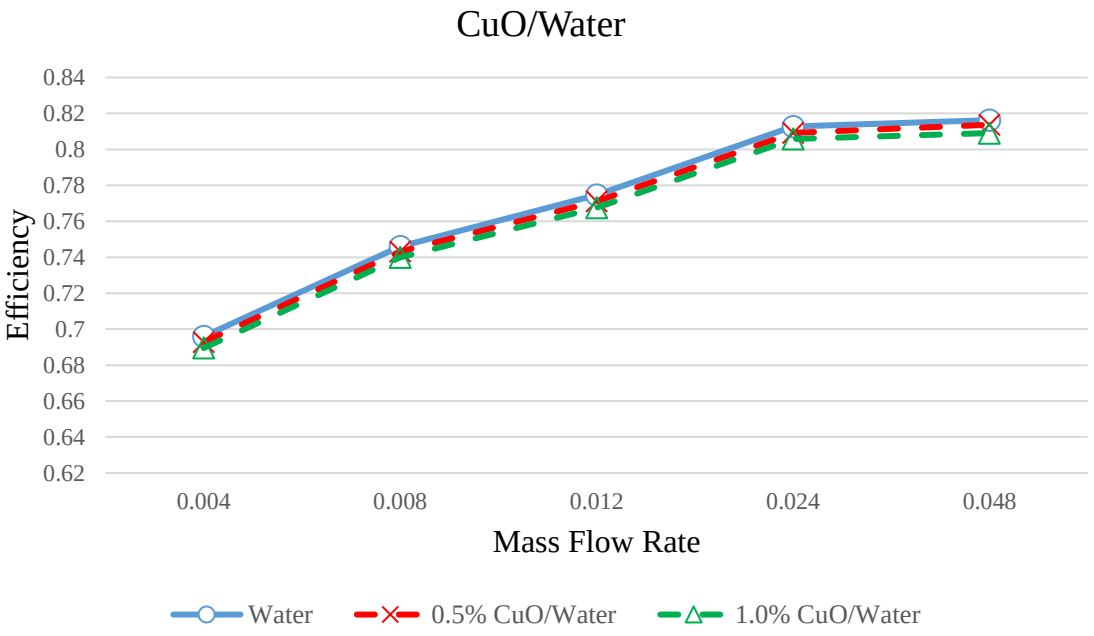

Figure 21. Efficiency of FPSC when CuO/Water as the working fluid

Figure 22 shows the result of the experimental study of Arıkan et al. [60], who used different nanofluids, such as Al_2O_3 and ZnO in the FPSCs. When Al_2O_3 was used in their study, the results showed that using nanoparticles as the working fluid yielded better efficiency compared with the use of water. In the simulation result of the current study, the efficiency when nanofluid was used as the working fluid is lower than when water was used because of the limitation discussed above. The experimental results of Arikan et al. [60] showed the efficiency could actually be improved by using nanoparticles.

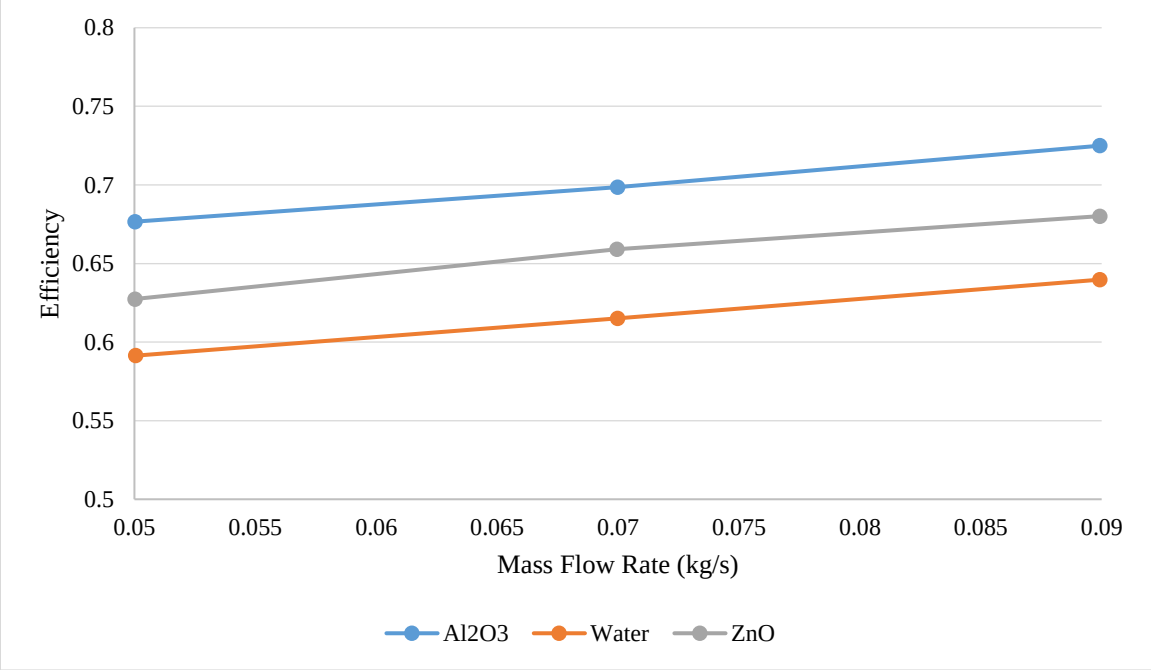

Figure 22. Experimental curves for nanofluids [60]

Khudhayer et al. [61] experimentally compared the performance of FPSCs nanofluid and water as the working fluids. In Table 4, the results show that the efficiency

for 0.1% of TiO_2/water efficiency was 4% higher than that for water at the same mass flow rate, and 0.1% of CuO/water showed the best performance of all, which was 5% higher than that for water. This research also shows that the addition of nanoparticles into the water can enhance the efficiency of solar collectors.

Type of fluid	**Mass flow rate**	**Efficiency (%)**
Water	1.5 L/min	50
Nanofluid (TiO2-0.1%)	1.5 L/min	54
Nanofluid (CuO-0.1%)	1.5 L/min	55

Table 4. Experimental resutls for FPSCs with different nanofluids [61]

Ekramian et al. [62] performed a numerical simulation to predict the thermal efficiency of water and several types of nanofluid, such as Al_2O_3/water and CuO/water. Figures 23 and 24 show that nanofluids enhanced the thermal efficiency of the solar collector. The higher the weight fraction of nanoparticles, the higher was the efficiency. The results show that CuO/water with wt%=3 showed the best performance among all working fluids.

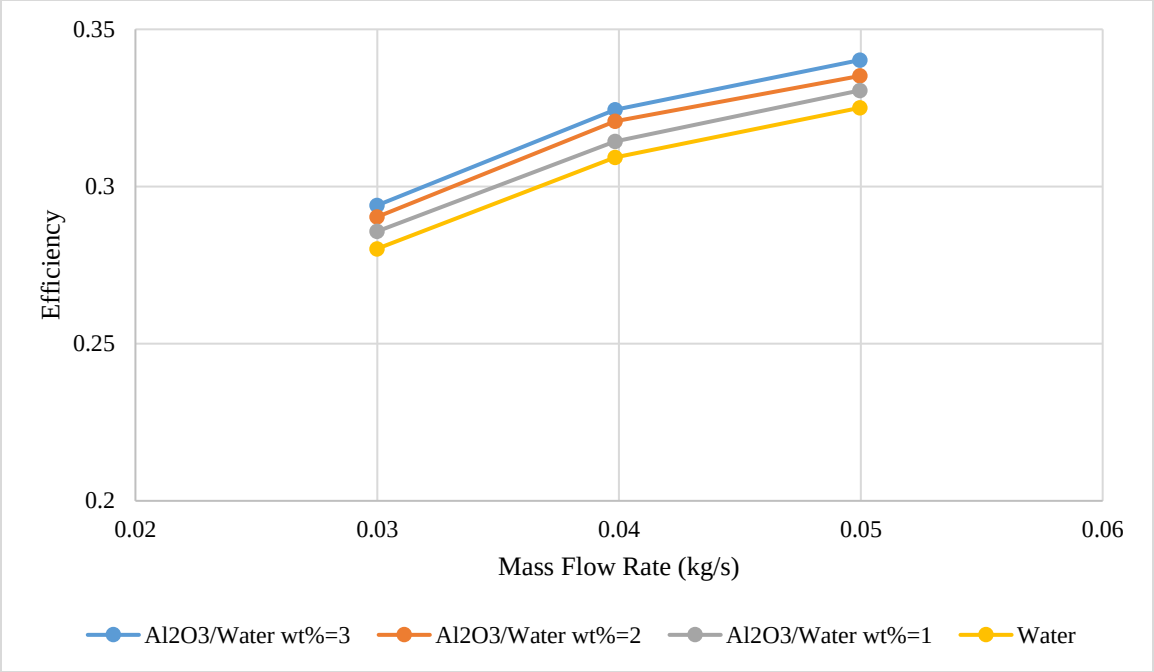

Figure 23. Thermal efficiency of Al_2O_3/water vs. mass flow rate [62]

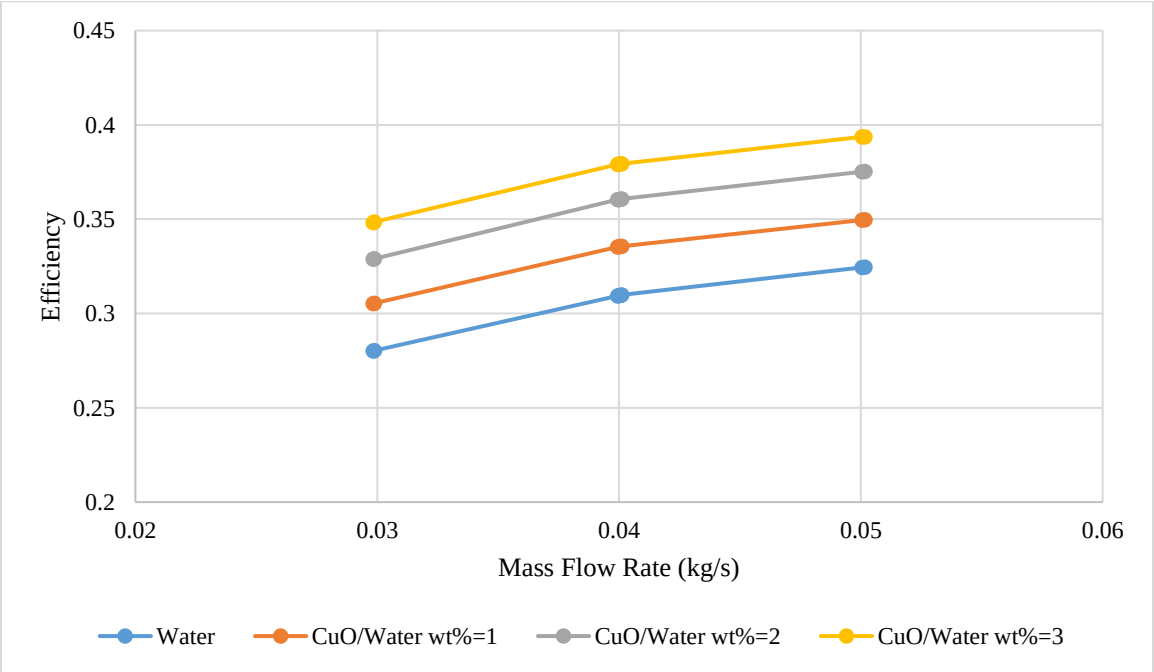

Figure 24. Thermal efficiency of CuO/water vs. mass flow rate [62]

4.3 Pressure drop and pumping power

In the simulation, there were two derived values of pressure in the model, one for inlet, and the other for outlet. The difference between these two boundary conditions was the pressure drop.

Instead of using mass flow rate, the volume flow rate was set to 0.000004 m^3/s. Figure 25 shows the pressure drop for the five different working fluids, and evidently, with a higher volume concentration of nanoparticles, the pressure drop was larger.

In Figure 26, the result shows the pressure drop difference (%) for Al_2O_3/water and CuO/water compared with water. The higher the particle volume fraction, the larger was the pressure drop difference.

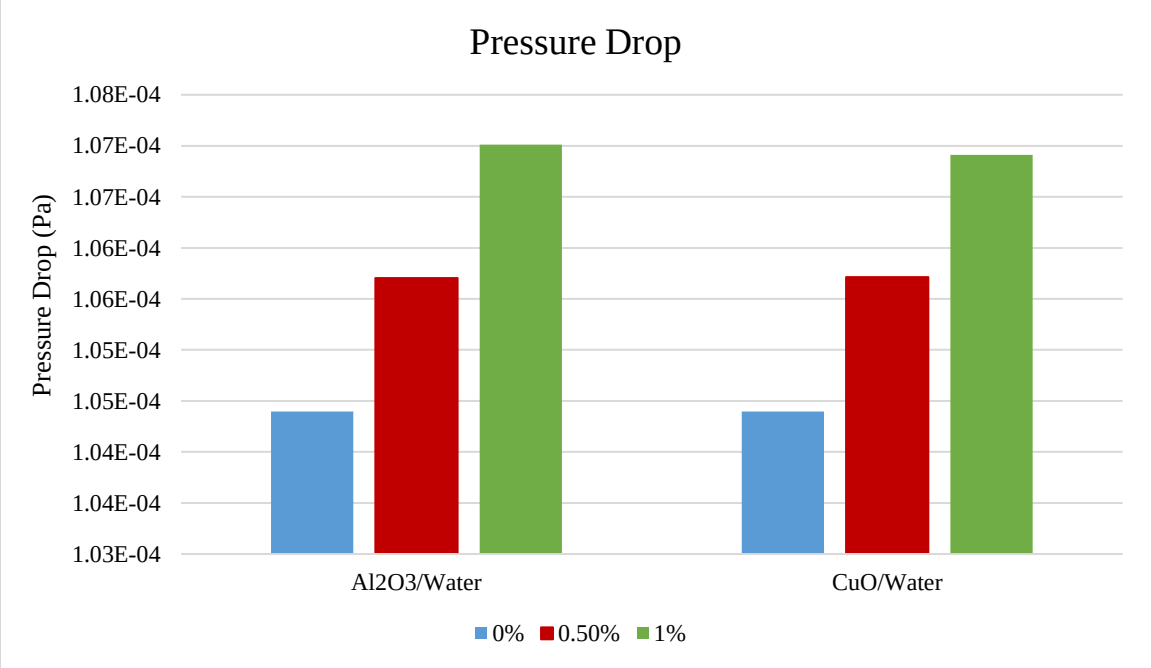

Figure 25. Pressure Drop ΔP of FPSC

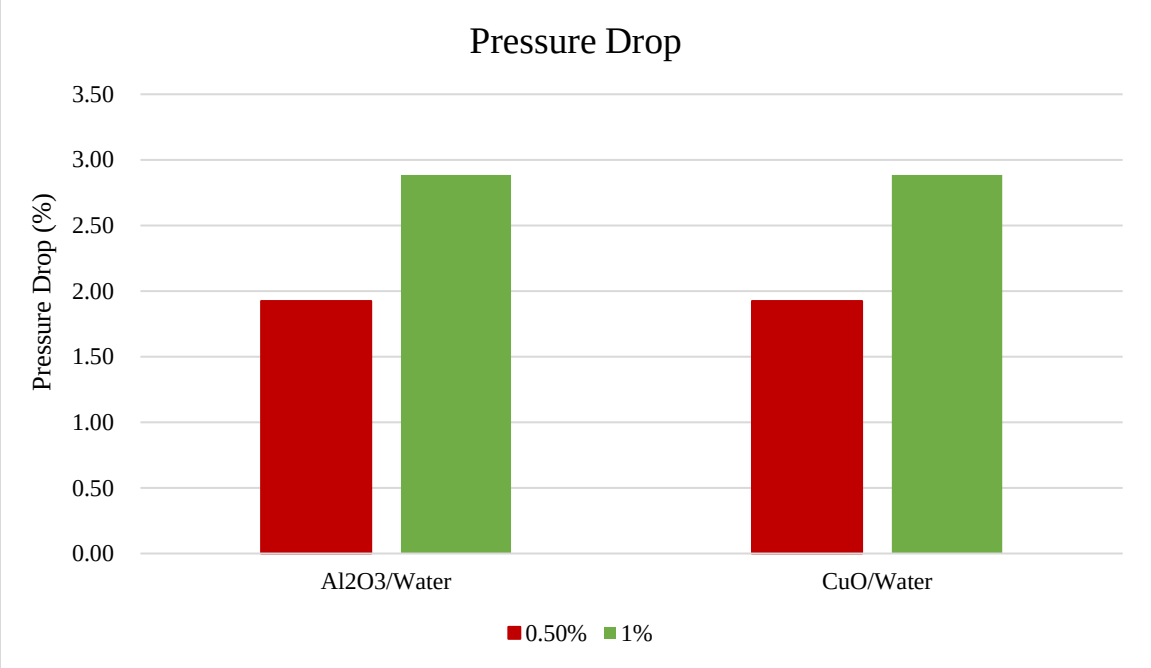

Figure 26. Comparison of ΔP Al_2O_3 and CuO nanofluids with that of water (%)

Equation (11) in chapter III to calculate the pumping power in the simulation. The results is shown in Figure 27 and Figure 28

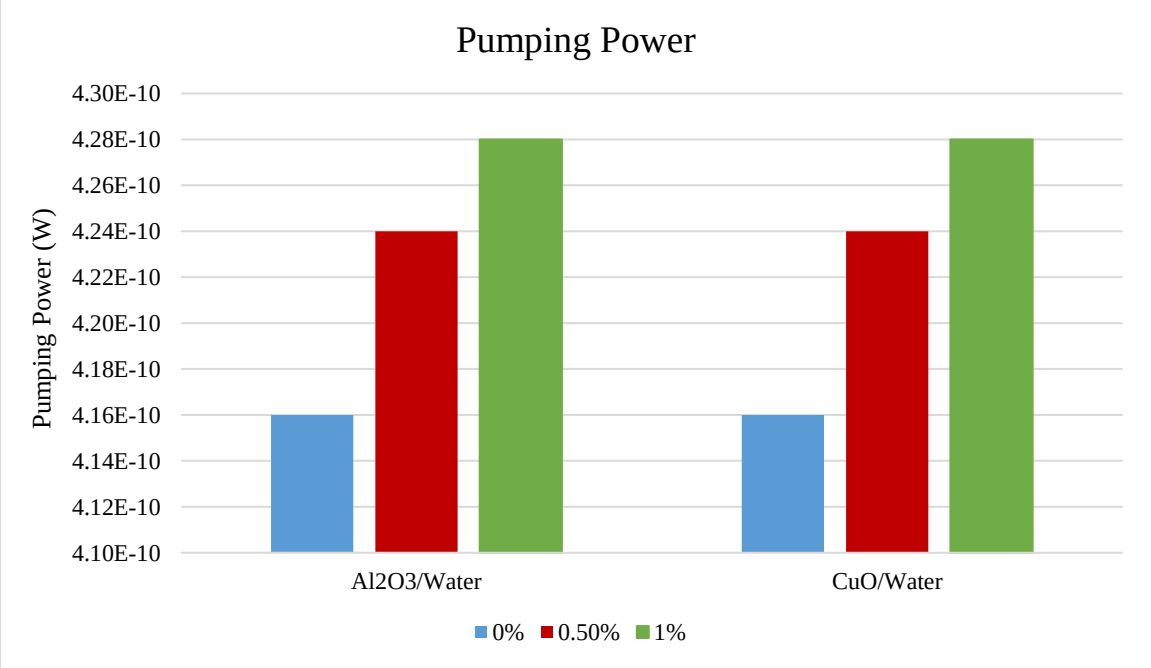

Figure 27. Pumping Power of FPSC

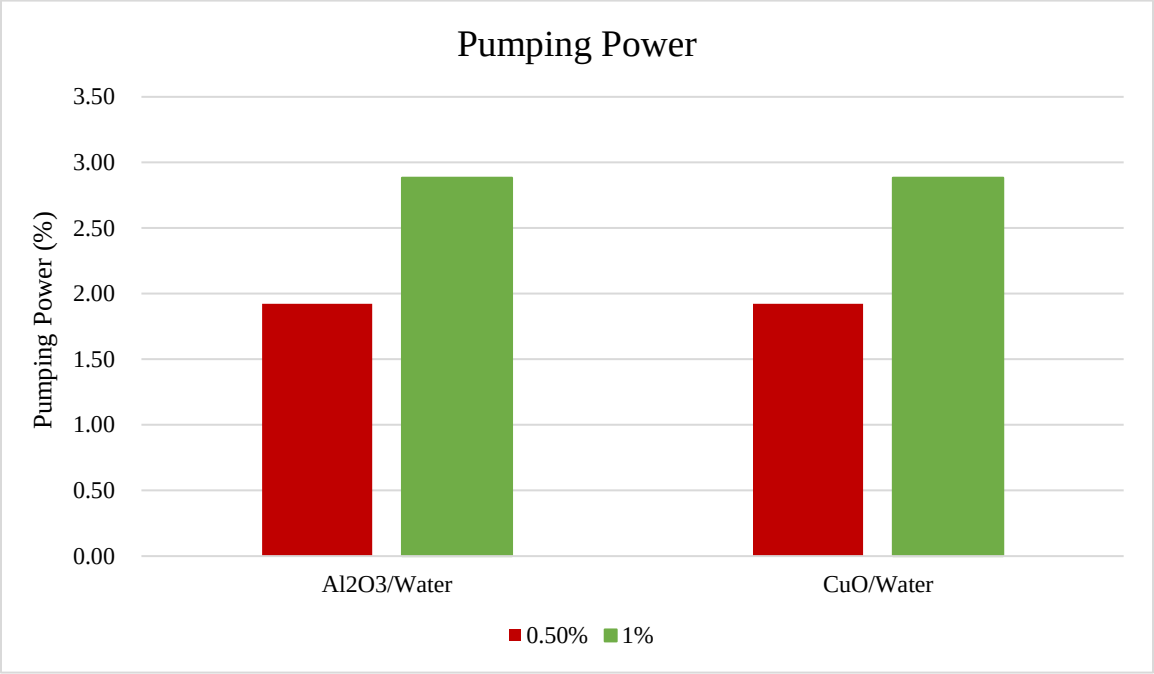

Figure 28. Comparison of ΔP of Al_2O_3 and CuO nanofluids with that of water (%)

Some other researches have verified that adding nanoparticles to the base fluid would influence the pressure drop and the pumping power of FPSCs.

Verma et al. [63] tried several types of nanofluids as the working fluid of FPSCs with a 0.025 kg/s flow rate. Figure 29 shows that the addition of nanoparticles to the water increased the pumping power loss ratio. The CuO/water showed the best performance of all.

Alim et al. [64] analyzed the influence of nanofluids in an FPSC. In Figures 30 and 31, the results show that the addition of nanoparticles to the base fluid increased the pressure drop and the pumping power, and the CuO/water nanofluid had an extra penalty og 1.58% in the pumping power.

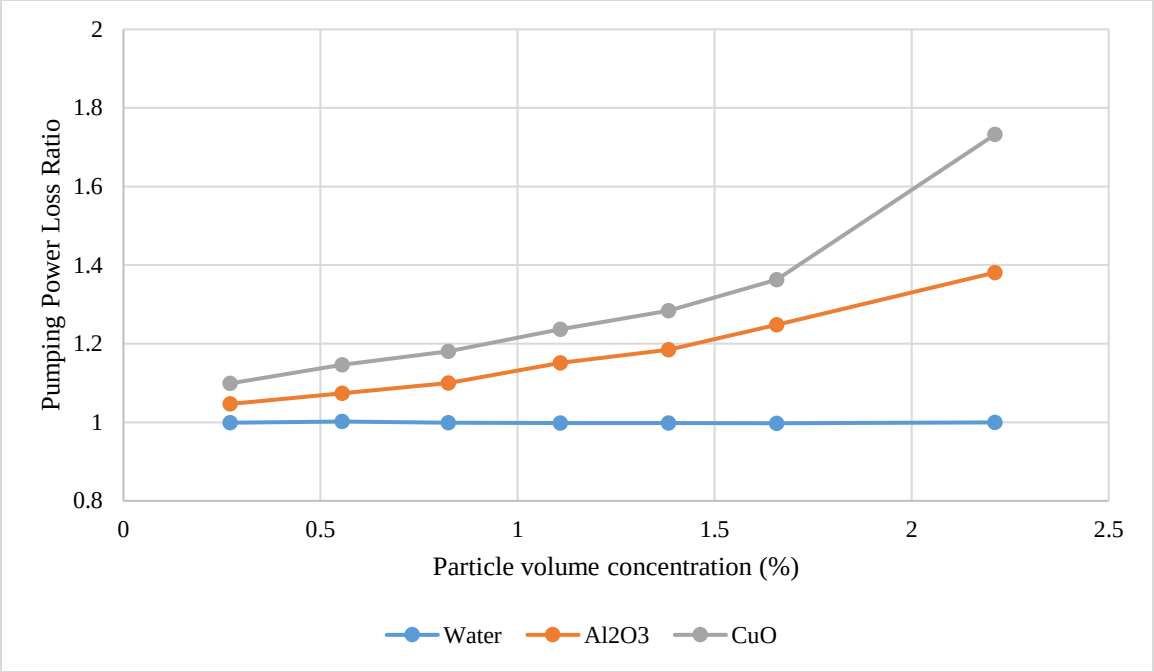

Figure 29. Particle volume concentration vs. pumping power loss ratio [63]

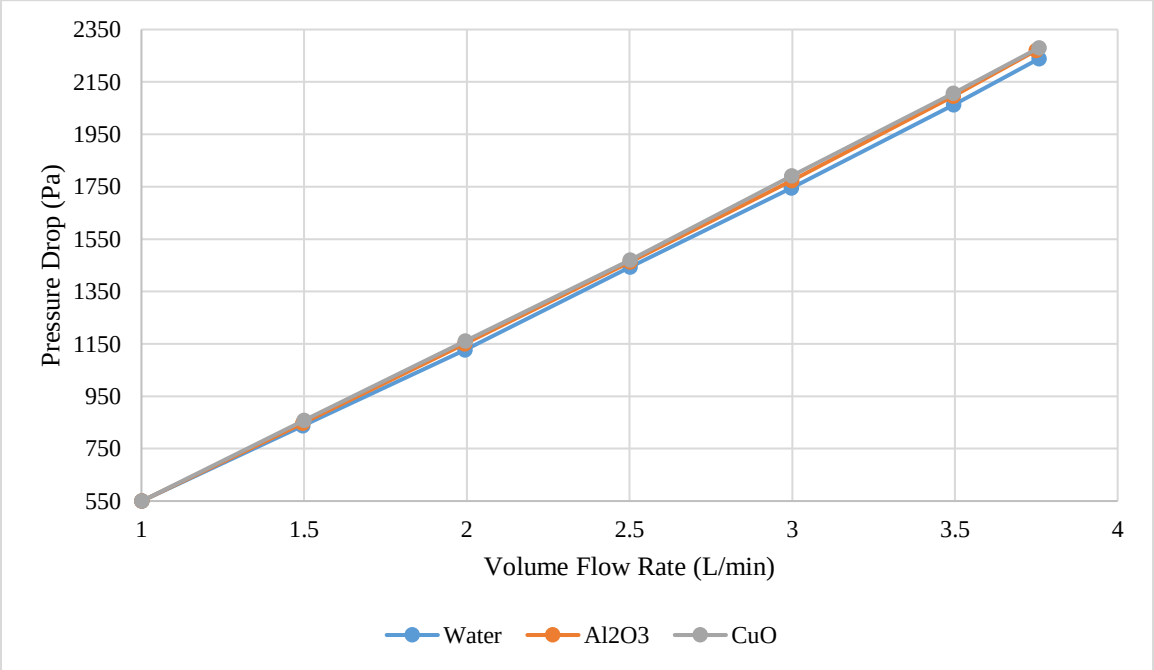

Figure 30. Volume flow rate vs. pressure drop

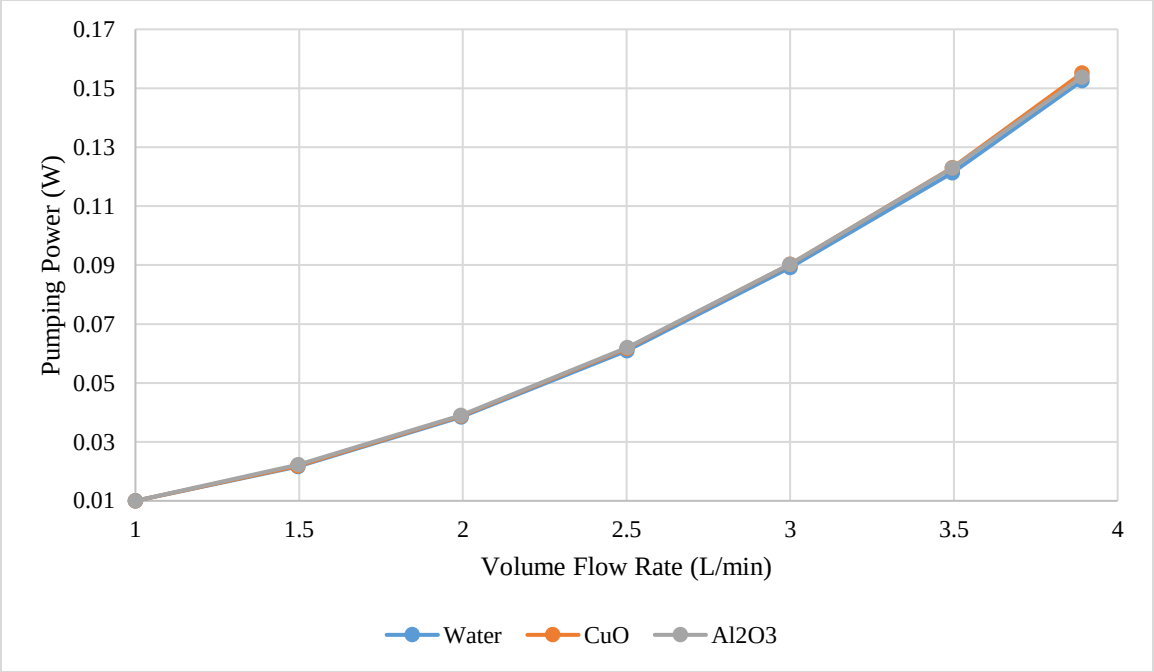

Figure 31. Volume flow rate vs. pumping power

The higher the volume concentration of nanoparticles, the larger the pressure drop. The flow rate in this simulation was constant, therefore, the higher the pressure drop, the higher was the pumping power.

Figure 32 includes the pressure contours of 0%, 0.5%, and 1% of Al_2O_3/water. Figure 33 includes the pressure contours of 0%, 0.5%, and 1% of CuO/water.

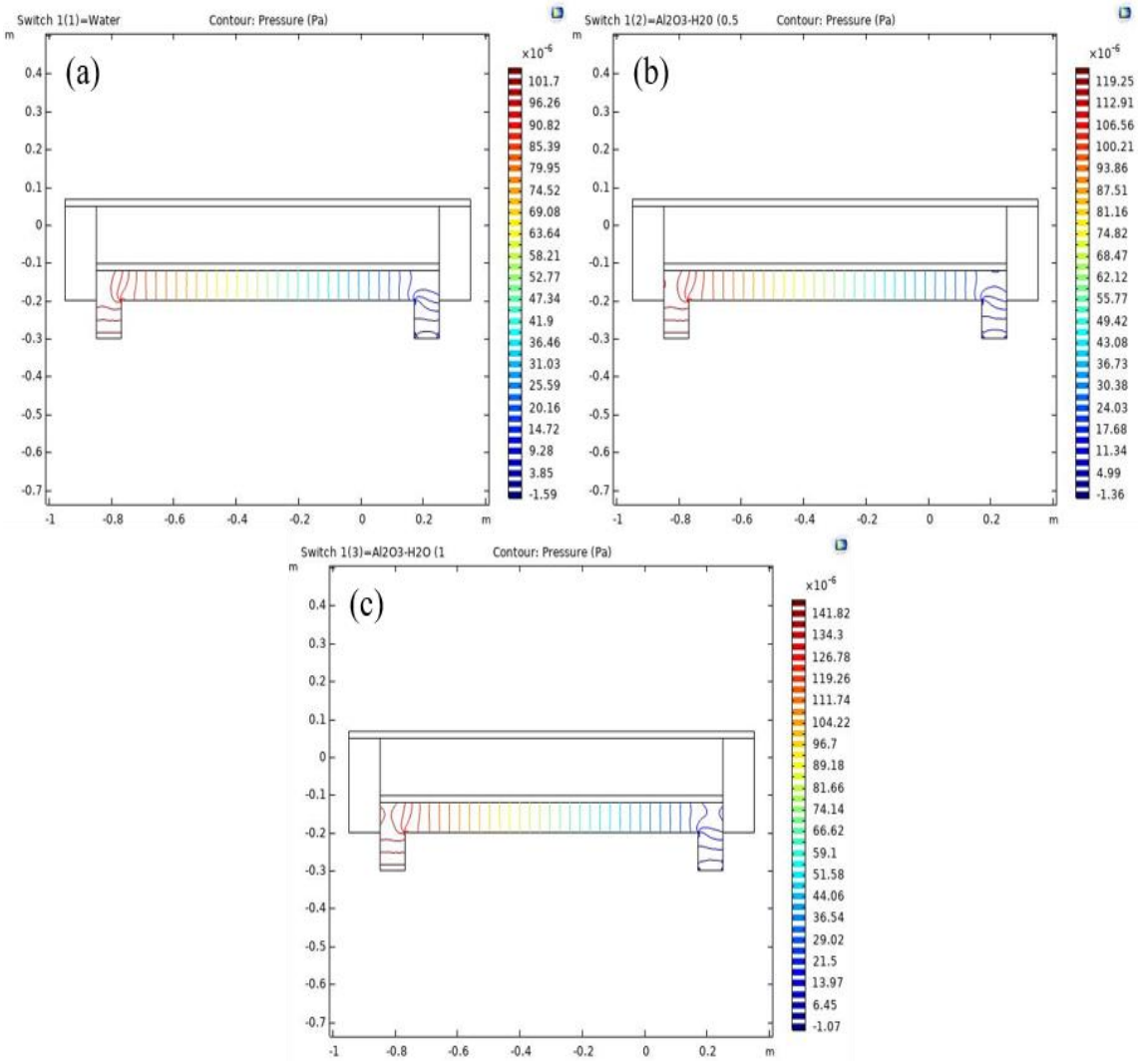

Figure 32. Pressure contours of Al_2O_3/water for (a) 0% (b) 0.5% (c) 1%

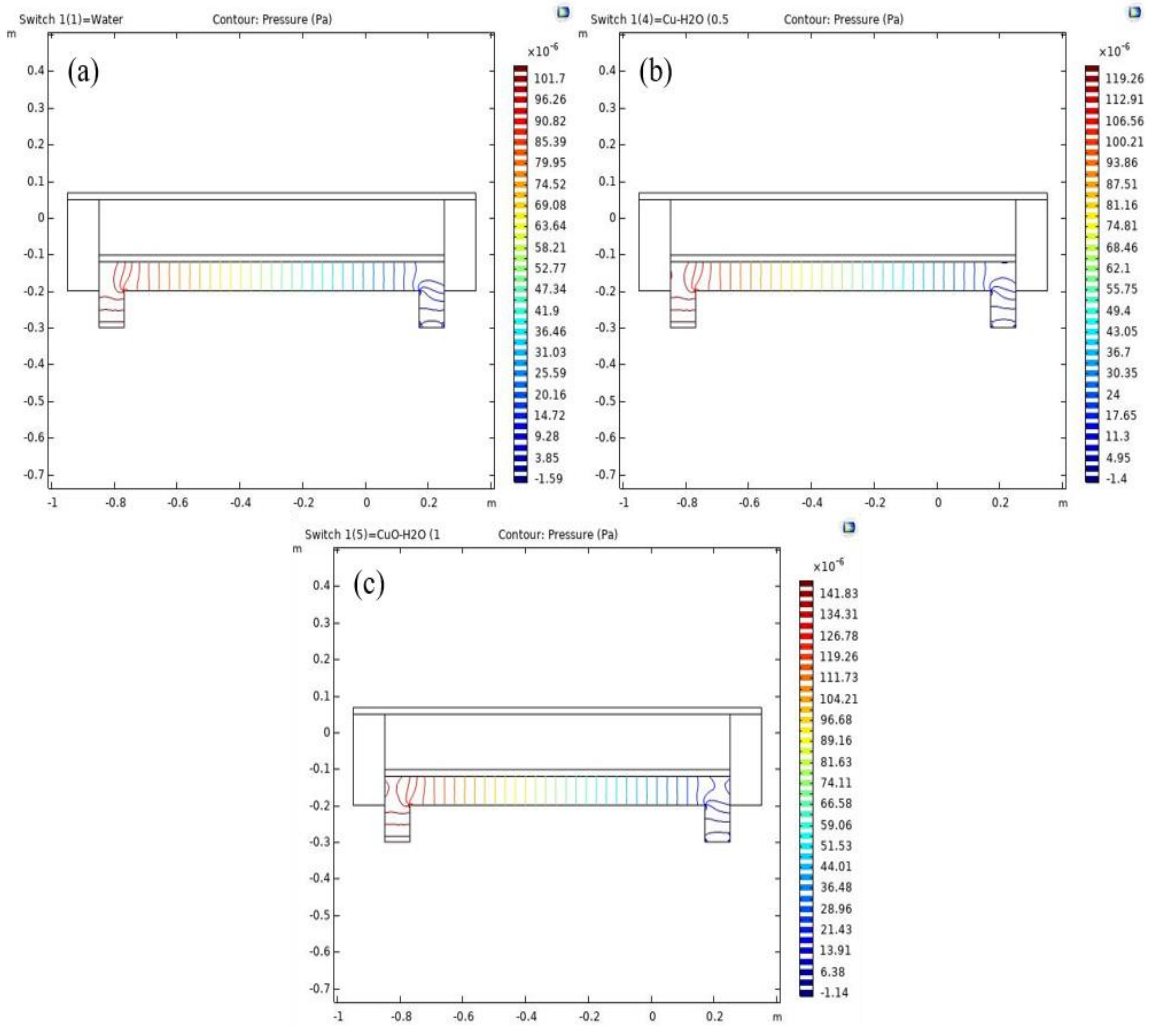

Figure 33. Pressure contours of CuO/water for (a) 0% (b) 0.5% (c) 1%

Chapter V

Conclusion

With the increase in environmental awareness, renewable energy development has assumed importance, and solar energy has a significant role in this task; Many researchers have devoted efforts to enhancing the efficiency of solar energy conversion and storing energy more effectively.

Among many existing methods that have helped improve the development of solar energy, the use of nanofluids has attracted the attention of researchers. After Choi & Eastman [8] presented their innovative idea of using nanofluids to enhance heat transfer, many studies have examined the use of novel nanofluids, and there have been numerous papers discussing how nanofluids improve the solar collector system and the development of future work.

The addition of nanoparticles to the working fluid (water) of the solar collector is one of the methods to enhance the solar collector's performance.

In this research, two types of nanoparticles were used: Al_2O_3 and CuO. These two materials have been the most used nanoparticles in recent studies, and CuO has shown outstanding performance in enhancing the ratio of heat transfer. Three different volume concentrations were used, 0% (base fluid), 0.5%, and 1%. The base fluid used n the simulation was water.

After the exact boundary conditions were specified in COMSOL, the simulation was conducted satisfactorily.

The results can be discussed under three different categories: outlet temperature, efficiency, and pressure drop.

In Figures 15, 16, and 17, working fluids with a larger volume concentration of nanoparticles show a considerably higher outlet temperature. When the working fluid was water, the outlet temperature was 333.53 K. For 0.5% and 1% of Al_2O_3 nanoparticles, the outlet temperature was 333.99 K and 334.43 K, respectively; for 0.5% and 1% of CuO nanoparticles, the outlet temperature was 334.36 K and 335.18 K, respectively. With the addition of nanoparticles, the specific heat C_P decreases, which can explain why nanofluid has a higher outlet temperature when it is used as the working fluid. The temperature difference percentage (ΔT %) for 1% of Al_2O_3 and 1% of CuO relative to water reached 2.4 % and 4.7%. In particular, CuO showed a better performance than Al_2O_3.

The results showed that adding nanoparticles to water and then using the water as nanofluid slightly decreased the efficiency of the flat plate solar collector owing to limitations such as the absorption and reflection rates of nanoparticles being ignored in the simulation and constraints in the design of the model. However, the efficiency of the solar collector increased noticeably with the mass flow rate.

The charts in Figures 25 and 26 show that the addition of nanoparticles influenced the pressure drop compared to water. For a higher volume concentration of nanoparticles, the pressure drop was higher. The difference between Al_2O_3 and CuO was not apparent; however, the pressure drop for 0.5% nanofluid was greater than that for the base fluid by almost 2%, and the pressure drop for the 1% nanofluid was greater than that for the base

fluid by almost 3%. The volume flow rate was constant in this study. In Figure 27 and Figure 28, a higher pressure drop corresponds to a higher pumping power.

The results accorded with the theory that nanofluids effectively enhance the ratio of heat transfer. The use of nanofluids can improve the efficiency of the solar collector, which might be one of the solutions to face the energy crisis. Additional research is necessary to make this technique widely used. However, the present study showed this technique to be promising, and the day of success can be expected soon.

References

1. Administration, U.S.E.I. *What is U.S. electricity generation by energy source?* 2019; Available from: https://www.eia.gov/tools/faqs/faq.php?id=427&t=3.
2. SEIA. *Solar Energy*. 2020; Available from: https://www.seia.org/initiatives/about-solar-energy.
3. Boyle, M. *Which country uses the most solar power? The top 10 solar-powered nations.* 2019; Available from: https://www.finder.com/uk/nation-most-solar-power.
4. Kazmeyer, M., *Future of Solar Power: Obstacles & Problems.* 2018.
5. Jordan Hanania, K.S., Brodie Yyelland, Jason Donev. *Solar Collector*. 2018; Available from: https://energyeducation.ca/encyclopedia/Solar_collector.
6. Ksenya. *Types of Solar Thermal Collectors*. 2011; Available from: https://solartribune.com/solar-thermal-collectors/.
7. Nasir El Bassam, P.M.a.M.L.S., *Distributed Renewable Energies for Off-Grid Communities-Strategies and Technologies toward Achieving Sustainability in Energy Generation and Supply*. 2013, Elsevier.
8. Choi, S.U. and J.A. Eastman, *Enhancing thermal conductivity of fluids with nanoparticles*. 1995, Argonne National Lab., IL (United States).
9. Abdul Kaggwa, J.K.C., *Developments and future insights of using nanofluids for heat transfer enhancements in thermal systems: a review of recent literature.* International Nano Letters, 2019.
10. Yimin Xuan, Q.L., *Heat transfer enhancement of nanofluids.* International Journal of Heat and Fluid Flow, 2000.
11. Naser Ali, J.A.T., Abdulmajid Addali, *A review on nanofluids: fabrication, stability, and thermophysical properties.* Journal of Nanomaterials, 2018.
12. Chaudhari, S.S., R. R. Chakule, and P. S. Talmale, *Experimental study of heat transfer characteristics of Al2O3 and CuO nanofluids for machining application.* Materials Today: Proceedings 2019: pp. 788-797.
13. Phor, L., et al., *Al 2 O 3-Water Nanofluids for Heat Transfer Application.* MRS Advances 4.28-29 2019: p. 1611-1619.
14. Rafi, A.A., et al, *Experimental analysis of heat transfer with CuO, Al2O3/water-ethylene glycol nanofluids in automobile radiator.* AIP Conference Proceedings. Vol. 2121. No. 1. AIP
15. PVenkitaraj, K.P., and S. Suresh, *Effects of Al2O3, CuO and TiO2 nanoparticles son thermal, phase transition and crystallization properties of solid-solid phase change material.* Mechanics of Materials 128, 2019: p. 64-88.
16. Sivasubramanian, M., T. Theivasanthi, and R. Manimaran, *Experimental investigation on heat transfer enhancement in a minichannel using CuO-water nanofluid.* International Journal of Ambient Energy, 2019. 40(8): pp. 847-853.

17. Zheng, M., et al., *Effect of Al 2 O 3/water nanofluid on heat transfer of turbulent flow in the inner pipe of a double-pipe heat exchanger.* Heat and Mass Transfer, 2019: pp. 1-14.
18. Sulgani, M.T., and Arash Karimipour, *Improve the thermal conductivity of 10w40-engine oil at various temperature by addition of Al2O3/Fe2O3 nanoparticles.* Journal of Molecular Liquids, 2019. 283: pp. 660-666.
19. Yu, W., et al., *Significant thermal conductivity enhancement for nanofluids containing graphene nanosheets.* Physics Letters A, 2011. **375**(10): p. 1323-1328.
20. Sen Gupta, S., et al., *Thermal conductivity enhancement of nanofluids containing graphene nanosheets.* Journal of Applied Physics, 2011. **110**(8): p. 084302.
21. Aggarwal, V. *What are the most efficient solar panels on the market? Solar panel cell efficiency explained*. 2020; Available from: https://news.energysage.com/what-are-the-most-efficient-solar-panels-on-the-market/.
22. Rajneesh Kumar, A.K., and Varun Goel, *Performance improvement and development of correlation for friction factor and heat transfer using computational fluid dynamics for ribbed triangular duct solar air heater.* Renewable Energy, 2019. **131**: pp. 788-799.
23. Liu, D., et al., *SnO2-based perovskite solar cells: configuration design and performance improvement.* Solar RRL, 2019. **3**(2): p. 1800292.
24. Rezaei, B., Irannejad, N., Ensafi, A. A., & Kazemifard, N, *The impressive effect of eco-friendly carbon dots on improving the performance of dye-sensitized solar cells.* Solar Energy, 2019. **182**: p. 412-419.
25. Jiang, C., et al., *Alkali Metals Doping for High-Performance Planar Heterojunction Sb2S3 Solar Cells.* Solar RRL, 2019. **3**(1): p. 1800272.
26. Ebrahimi, M., et al., *Performance enhancement of mesoscopic perovskite solar cells with GQDs-doped TiO2 electron transport layer.* Solar Energy Materials and Solar Cells, 2020. **208**: p. 110407.
27. Sarafraz, M., et al., *Potential of solar collectors for clean thermal energy production in smart cities using nanofluids: experimental assessment and efficiency improvement.* Applied Sciences, 2019. **9**(9): p. 1877.
28. Nazari, S., H. Safarzadeh, and M. Bahiraei, *Performance improvement of a single slope solar still by employing thermoelectric cooling channel and copper oxide nanofluid: an experimental study.* Journal of cleaner production, 2019. **208**: p. 1041-1052.
29. Sözen, A., A. Khanları, and E. Çiftçi, *Experimental and numerical investigation of nanofluid usage in a plate heat exchanger for performance improvement.* Int J Renew Energy Dev, 2019. **8**(1): pp. 27-32.
30. Malekan, M., A. Khosravi, and S. Syri, *Heat transfer modeling of a parabolic trough solar collector with working fluid of Fe3O4 and CuO/Therminol 66 nanofluids under magnetic field.* Applied Thermal Engineering, 2019. **163**: p. 114435.
31. Vakili, M., et al., *Experimental investigation of graphene nanoplatelets nanofluid-based volumetric solar collector for domestic hot water systems.* Solar Energy, 2016. **131**: pp. 119-130.

32. Iranmanesh, S., et al., *Thermal performance enhancement of an evacuated tube solar collector using graphene nanoplatelets nanofluid.* Journal of cleaner production, 2017. **162**: pp. 121-129.
33. Sharafeldin, M., et al., *Evacuated tube solar collector performance using copper nanofluid: Energy and environmental analysis.* Applied Thermal Engineering, 2019. **162**: p. 114205.
34. Bellos, E. and C. Tzivanidis, *Thermal efficiency enhancement of nanofluid-based parabolic trough collectors.* Journal of Thermal Analysis and Calorimetry, 2019. **135**(1): pp. 597-608.
35. Dehaj, M.S. and M.Z. Mohiabadi, *Experimental investigation of heat pipe solar collector using MgO nanofluids.* Solar Energy Materials and Solar Cells, 2019. **191**: pp. 91-99.
36. Sayigh, A.A.M., *4 - Liquid Heaing Solar Flat Plate Collectors.* Solar Energy Conversion II, 1981: pp. 41-56.
37. A.A.M.Sayigh, *4 - The Technology of flat plate collectors.* Solar Energy Conversion 1979: p. 101-124.
38. S.C.Bhatia, *4 - Solar thermal energy.* Advanced Renewable Energy Systems, 2014: pp. 94-193.
39. J.C.McVEIGH, *CHAPTER 3 - Water and air heating applications.* Sun Power (Second Edition), 1983: pp. 25-64.
40. Tutorials, A.E. *Flat Plate Collector*. 2020; Available from: http://www.alternative-energy-tutorials.com/solar-hot-water/flat-plate-collector.html.
41. Jouybari, H.J., M.E. Nimvari, and S. Saedodin, *Thermal performance evaluation of a nanofluid-based flat-plate solar collector.* Journal of Thermal Analysis and Calorimetry, 2019. **137**(5): pp. 1757-1774.
42. Saffarian, M.R., M. Moravej, and M.H. Doranehgard, *Heat transfer enhancement in a flat plate solar collector with different flow path shapes using nanofluid.* Renewable Energy, 2020. **146**: pp. 2316-2329.
43. Stalin, P.M.J., et al., *Experimental and theoretical investigation on the effects of lower concentration CeO 2/water nanofluid in flat-plate solar collector.* Journal of Thermal Analysis and Calorimetry, 2019. **135**(1): pp. 29-44.
44. Arora, S., G. Fekadu, and S. Subudhi, *Energy and Exergy Analysis of Marquise Shaped Channel Flat Plate Solar Collector Using Al2O3–Water Nanofluid and Water.* Journal of Solar Energy Engineering, 2019. **141**(4).
45. Akram, N., et al., *An experimental investigation on the performance of a flat-plate solar collector using eco-friendly treated graphene nanoplatelets–water nanofluids.* Journal of Thermal Analysis and Calorimetry, 2019. **138**(1): pp. 609-621.
46. Nasrin, R. and M. Alim, *Finite Element Simulation of Forced Convection in a Flat Plate Solar Collector: Influence of Nanofluid with Double Nanoparticles.* Journal of Applied Fluid Mechanics, 2014. **7**(3).
47. Mohammad Reza Safaei, A.J., Ali Kianifar, Samira Gharehkhani, Akeel Shebeeb Kherbeet, Marjan Goodarzi and Mahidzal Dahari, *Mathematical Modeling for Nanofluids Simulation: A Review of the Latest Works.* 2016.

48. Esfandiary, M., A. Habibzadeh, and H. Sayehvand, *Numerical Study of Single Phase/Two-Phase Models for Nano fluid Forced Convection and Pressure Drop in a Turbulence Pipe Flow.* 2016.
49. Jiji, L.M. and L.M. Jiji, *Heat convection*. 2006: Springer.
50. Xuan, Y. and Q. Li, *Heat transfer enhancement of nanofluids.* International Journal of heat and fluid flow, 2000. **21**(1): pp. 58-64.
51. Mondragón, R., et al., *Flat plate solar collector performance using alumina nanofluids: Experimental characterization and efficiency tests.* PloS one, 2019. **14**(2).
52. Einstein, A., *Eine neue bestimmung der moleküldimensionen*. 1905, ETH Zurich.
53. Udawattha, D.S., M. Narayana, and U.P. Wijayarathne, *Predicting the effective viscosity of nanofluids based on the rheology of suspensions of solid particles.* Journal of King Saud University-Science, 2019. **31**(3): pp. 412-426.
54. Kitano, T., T. Kataoka, and T. Shirota, *An empirical equation of the relative viscosity of polymer melts filled with various inorganic fillers.* Rheologica Acta, 1981. **20**(2): pp. 207-209.
55. Al-Kouz, W., et al., *Entropy generation optimization for rarified nanofluid flows in a square cavity with two fins at the hot wall.* Entropy, 2019. **21**(2): p. 103.
56. Rehena Nasrin, S.P., M.A. Alim, Ali J. Chamkha, *Non-darcy forced convection thorugh a wavy porous channel using CuO nanofluid* International Journal of Energy & Technology, 2012. **4 (8)**: pp. 1-8.
57. Nejad, M.B., et al. *Influence of nanofluids on the efficiency of Flat-Plate Solar Collectors (FPSC)*. in *E3S Web of Conferences*. 2017. EDP Sciences.
58. WIKIPEDIA. *Boundary conditions in fluid dynamics*. 2019; Available from: https://en.wikipedia.org/wiki/Boundary_conditions_in_fluid_dynamics.
59. Bakker, A. *Lecture 7 - Meshing*. Applied Computational Fluid Dynamics 2002; Available from: http://www.bakker.org/dartmouth06/engs150/07-mesh.pdf.
60. Arıkan, E., S. Abbasoğlu, and M.J.S. Gazi, *Experimental performance analysis of flat plate solar collectors using different nanofluids.* 2018. **10**(6): p. 1794.
61. Khudhayer, W.J., et al., *Enhanced Heat Transfer Performance of a Flat Plate Solar Collector using CuO/water and TiO2/water Nanofluids.* 2018. **13**(6): pp. 3673-3682.
62. Ekramian, E., et al., *Numerical investigations of heat transfer performance of nanofluids in a flat plate solar collector.* 2014. **2**: pp. 30-39.
63. Verma, S.K., et al., *Experimental evaluation of flat plate solar collector using nanofluids.* 2017. **134**: pp. 103-115.
64. Alim, M.A., et al., *Analyses of entropy generation and pressure drop for a conventional flat plate solar collector using different types of metal oxide nanofluids.* 2013. **66**: pp. 289-296.